Review

Vu, Van Tuan; Delgado-Saborit, Juana Maria; Harrison, Roy M.

DOI:
10.1016/j.atmosenv.2015.09.027

Document Version
Peer reviewed version

Citation for published version (Harvard):
Vu, VT, Delgado-Saborit, JM & Harrison, RM 2015, 'Review: Particle number size distributions from seven major sources and implications for source apportionment studies', *Atmospheric Environment*, vol. 122, pp. 114-132. https://doi.org/10.1016/j.atmosenv.2015.09.027

REVIEW: PARTICLE NUMBER SIZE DISTRIBUTIONS FROM SEVEN MAJOR SOURCES AND IMPLICATIONS FOR SOURCE APPORTIONMENT STUDIES

Tuan V. Vu, Juana Maria Delgado-Saborit, and Roy M. Harrison[1*†]

Division of Environmental Health & Risk Management

School of Geography, Earth & Environmental Sciences

University of Birmingham

Edgbaston, Birmingham B15 2TT

United Kingdom

[*] To whom correspondence should be addressed.
Tele: +44 121 414 3494; Fax: +44 121 414 3708; Email: r.m.harrison@bham.ac.uk

[†]Also at: Department of Environmental Sciences / Center of Excellence in Environmental Studies, King Abdulaziz University, PO Box 80203, Jeddah, 21589, Saudi Arabia

HIGHLIGHTS

- Particle number size distributions (PNSD) of seven major sources of urban particles
- Influence of atmospheric physical processes upon PNSD changes
- Implications of PNSD datasets for source identification
- A summary of current source apportionment studies of particle number in cities

ABSTRACT

The particle number size distribution (PNSD) of airborne particles not only provides us with information about sources and atmospheric processing of particles, but also plays an important role in determining regional lung dose. As a result, urban particles and their size distributions have received much attention with a rapid increase of publications in recent years. The object of this review is to synthesise and analyse existing knowledge on particles in urban environments with a focus on their number concentration and size distribution. This study briefly reviews the characterization of PNSD from seven major sources of urban particles including traffic emissions, industrial emissions, biomass burning, cooking, transported aerosol, marine aerosol and nucleation. It then discusses atmospheric physical processes such as coagulation or condensation which have a strong influence on PNSD. Finally, the implications of PNSD datasets for source modelling are briefly discussed. Based on this review, it is concluded that the concentrations, modal structures and temporal patterns of urban particles are strongly influenced by traffic emissions, which are identified as the main source of particle number in urban environments. Information derived from particle number size distributions is beginning to play an important role in source apportionment studies.

Keywords: Urban particles; number size distribution; source apportionment; human exposure

1. INTRODUCTION

Ambient aerosols are mixtures of primary particles emitted from anthropogenic activities (e.g. industries, transportation), and natural sources (e.g. marine, forest burning), and secondary particles formed by gas-to-particle conversion processes including nucleation and condensation. They exist in a wide range of sizes, with most particles by number having a particle diameter (Dp) in the range from a few nanometres to around one hundred micrometres (Harrison et al., 2000). In recent years, aerosols have been an intense area of study since they have been found to play an important role in climate regulation and human health, in which particle number size distribution (PNSD) is recognised as a key metric in determining regional lung deposition.

In atmospheric environments, the PNSD is ideally characterized by a multi-lognormal structure, usually based on four main modes: the nucleation mode (Dp < 30nm), the Aitken mode (30 nm< Dp< 100 nm), the accumulation mode (100 nm < Dp< 1 µm) and the coarse mode (Dp > 1 µm) (Harrison et al., 2000; Hussein et al., 2005; Kulmala et al., 2004; Von Bismarck-Osten et al., 2013). In an urban area, the majority of particles by number are typically found in the nucleation and Aitken modes, while the particle surface and volume or mass are found predominantly in the accumulation and coarse modes as shown in Figure 1. According to Seinfeld and Pandis (1998) a high percentage of urban particles is normally found in particles with diameters smaller than 0.1 µm, while the most common size ranges for particle surface area and particle mass are in the range of 0.1-0.5 µm and larger than 0.1 µm, respectively. More than 25% of total urban particle number counts are in the size range with diameter less than 10 nm, whilst particles with diameters less than 50 nm and 100 nm account for approximately 75% and 90% of the total number concentration in the studies reported by Stanier et al. (2004a) and Woo et al. (2001). Von Bismarck-Osten et al. (2013) reported that more than 80% of particles were observed in the nucleation and Aitken modes in five major European cities (as shown in Figure 2). Coarse particles do not contribute significantly

to the total number of particles, with number concentrations reported as ranging only from 0.59 to 8 particle cm^{-3} (Gao et al., 2011; Stanier et al., 2004a; Wu et al., 2008).

Particles in different modes derive from different sources or chemical and physical processes. For example, nucleation mode particles from a roadside site are formed though nucleation in the atmosphere after rapid cooling and dilution of emissions and condensation of supersaturated vapour. Aitken mode particles are suggested to be a mixture of condensed semi-volatiles onto a solid core. Accumulation mode particles from road vehicles are mainly generated from combustion of fuel and lubricant oil and by growth of Aitken mode particles. Coarse particles are mechanically generated from attrition processes and include wind-blown soil and sea spray. This diversity is reflected in the measured PNSDs, which vary widely in the atmosphere due to the combination of multiple sources, which generate particles with different sizes and concentration characteristics, and the atmospheric formation and transformation processes which influence the evolution of size distribution (Morawska et al., 1999). This can be useful as information upon sources and processes affecting particles can be extracted from observational data. For example, Harrison et al. (2011) ran a PMF model on a PSND dataset measured at Marylebone Road, London and this study successfully identified specific contributions of particles from several sources, including brake dust and re-suspension. In addition, Beddows et al. (2014) demonstrated clearly the dynamics of particle formation by application of cluster analysis to a PNSD data set measured from 24 background stations across Europe. Another example is illustrated by the study of Dusek et al. (2006), who suggested that PNSD can be a better metric to achieve an estimate of total cloud condensation nuclei than particle chemical composition.

In the aspect of human exposure studies, PNSD is also an essential parameter. Numerous articles have shown that the ability of particles to penetrate deeply into the lung, which may contribute to disease, depends upon their number size distribution (von Klot et al., 2005). ICRP (1994) developed

regional lung deposition curves based upon particle size. In some studies, the number concentration of ultrafine particle has been more closely associated with adverse health effects than the mass concentration (Peters et al., 1997). Although knowledge of which particle metric is the best predictor of adverse health outcomes is incomplete, an increasing number of studies have found associations with particle number (Atkinson et al., 2010; HEI_Review_Panel, 2013; Oberdörster et al., 2010; Zhang et al., 2009).

Since different types of sources generate particles with different sizes and concentration characteristics, it is of great importance to know the sources of particles to understand measured particle size distributions (Morawska et al., 1999). The specific characteristics of the modal structure of distributions, as well as the temporal patterns of particle generation from different sources imply that particle size distribution and concentration profiles may be utilised to identify the specific sources contributing to measured distributions of particles and to apportion sources of particles in urban areas. In the next section, we review the characteristics of PNSD emitted from seven major sources of particles including traffic emissions, industrial emission, biomass burning, cooking emissions, long-range transported aerosols and nucleation.

2. SOURCES AND CHARACTERISTIC SIZE DISTRIBUTIONS

2.1 Traffic Related Emissions

2.1.1 Vehicle exhaust emissions

Vehicle emissions are considered a major source of particles in the urban atmosphere. Particle emissions from vehicles can be generated directly in the engine during combustion of fuels or can be formed in the air by nucleation and condensation during dilution and cooling of the hot exhaust gaseous emissions from the tailpipe. The combustion-generated particles consist mostly of solid graphitic carbon with a smaller amount of metallic ash, hydrocarbons and sulphur compounds. These particles are found mainly as soot in the Aitken and accumulation modes with the size

ranging from 30 nm to 500 nm (Shi et al., 2000). The smaller sized mode of particles is believed to be formed by binary nucleation of H_2SO_4-H_2O or ternary nucleation of H_2SO_4-NH_3-H_2O, which comprises a small hydrated sulphuric acid core coated with condensed hydrocarbons (Meyer and Ristovski, 2007; Shi and Harrison, 1999; Tobias et al., 2001). This second group of particles is found predominantly in the nucleation mode (below 30 nm) (Morawska et al., 2008). The overall size distribution of both types of particles emitted from vehicles has been described by a unimodal or bimodal lognormal distribution, depending upon the type of engine (spark ignition and diesel engines), the types of fuel and fuel properties (e.g. sulphur content), the exhaust after-treatment devices, the vehicle use (vehicle operating modes, load and speed) (Li et al., 2013; Myung and Park, 2012; Shi and Harrison, 1999; Agarwal et al., 2015), the test method (chassis dynamometer test, on-road measurements, ground-fixed measurements and field measurements) and the atmospheric conditions (temperature, wind speed or humidity) (Carpentieri and Kumar, 2011; Casati et al., 2007; Charron and Harrison, 2003).

2.1.1.1 PNSD measurements in different test methods and vehicle types

Road vehicle-generated particle size distributions have been measured using different sampling methods, resulting in a large variation of observed PNSD spectra. Particle number distributions generated by diesel engines in chassis dynamometer tests and on-road measurements typically present a bimodal distribution including a nucleation and an accumulation soot mode. For example, Giechaskiel et al. (2005) reported that the size distribution of a diesel engine exhaust plume exhibits two peaks, one with a size less than 30 nm and one at a size larger than 50 nm. Harrison et al. (2011) made similar observations from size spectra disaggregated by Positive Matrix Factorization. The nucleation mode contains mainly new small particles which are believed to be formed from condensation on a sulphuric acid or ash particle nucleus, and the accumulation soot mode is the result of incomplete combustion of the diesel fuel which consists of pyrolytic elemental carbon (EC) and organic carbon (OC). The latter includes primarily aliphatic hydrocarbons, polycyclic

159 aromatic hydrocarbons and lubricant-derived ash-related species. On the contrary, particles emitted
160 from gasoline vehicles are generally less than 80 nm in diameter and their size distributions usually
161 display a unimodal structure. The size distribution profile of traffic-generated particles is shown in
162 Table 1.
163
164 In field measurements, traffic generated particles, which have been mostly measured at kerbside or
165 in a tunnel or street canyon, show the majority of particles in the nucleation and Aitken modes, with
166 a peak mode smaller than 30 nm as summarized in Table 2. Wehner et al. (2002) noted that the
167 particle count median diameter (CMD) measured in a street canyon was lower than the CMD
168 measured for gasoline and diesel vehicles in chassis dynamometer tests (40-70 nm). This could be
169 explained by the new particles formed from gaseous emissions from the tailpipe due to nucleation
170 of hydrocarbons. During this period, dilution ratio plays an important role in controlling the
171 saturation ratios which lead to nucleation (Kirchstetter et al., 1999). Shi and Harrison (1999)
172 showed that size distributions of particles in diesel exhaust were strongly dependent upon dilution
173 ratio. It has been reported that the concentration of traffic-generated nanopartices was found to be
174 greater in winter compared to summer (Jeong et al., 2004; Jeong et al., 2006; Wang et al., 2011b),
175 but it is unclear whether this is an effect of lower temperature or lesser dilution. At a kerbside site,
176 PNSDs emitted from vehicle exhausts can show a bimodal distribution (Morawska et al., 2008), but
177 the number of modes sometimes vary dependent on sampling conditions and local sources. Agus et
178 al. (2007) reported that the typical urban aerosol roadside particle distribution has been shown as
179 the sum of three log-normal distributions including nucleation, Aitken and accumulation modes,
180 while Lingard et al. (2006) found four modes in the size range 6-225 nm during rush hour
181 conditions at a UK urban roadside site. As the modes typically overlap, curve fitting is often
182 needed to identify the contributing modes (e.g. Lingard et al., 2006; Dall'Osto et al., 2011a ,b).
183

Emissions from ship and aircraft engines can show some similarity to automotive diesel emissions. Hallquist et al. (2012) found that PNSDs obtained for a selective catalytic reduction (SCR) equipped marine diesel engine in on-board measurements after dilution and cooling of exhaust gases show a bimodal distribution with two peak modes at around 12 nm and 30-40 nm. A similar result was found in a test rig study of a four-stroke marine diesel engine by Petzold et al. (2008) which showed a bimodal distribution with two peaks at 15 and 50 nm. However, in another study, PNSDs measured in the plumes of passenger ships showed unimodal size distributions with an average geometric mean diameter (GMD) of 38 nm (Jonsson et al., 2011). This study suggested that "for those conditions (initial real-world dilution + plume processes) there is either enough condensational sinks available suppressing nucleation by adsorption/ condensation or that coagulation is taking place leading to a decrease in number but preserved mass". For particles emitted from aircraft and airports, small particles with a size range of 10-40 nm were found to be dominant in most studies (Buonanno et al., 2012; Kinsey et al., 2010; Mazaheri et al., 2008; Rogers et al., 2005; Zhu et al., 2011). Herndon et al. (2008) observed a peak at about 65 nm from take-off plumes, and the mean particle size decreased to a smaller mode (about 25 nm) for idling engine plumes.

2.1.1.2 Effects of fuel types and properties

The type of fuel (e.g. gasoline, diesel or biofuel) has a significant effect not only on particle concentration but also on its size distribution. For example, Kasper et al. (2007) observed a mode at about 30-40 nm associated with plumes from a two-stroke marine engine when using marine diesel oil, and a smaller mode around 25 nm when using heavy fuel oil (HFO). In another study, Armas et al. (2012) investigated the impacts of alternative fuels such as liquefied petroleum gas, compressed natural gas or bio-gas and found that the use of ethanol blended fuels on urban buses can reduce by 50% the number of particles in the accumulation mode, but causes a significant increase of particle number concentration in the nucleation mode. A recent study which compared the particle number

size distributions of primary and secondary aerosols from a 20% biodiesel blend and mineral diesel fuel by Agarwal et al. (2013) found that there was a reduction of approximately two orders of magnitude in particle number due to an addition of 20% biodiesel to mineral diesel, which was attributed to the lower sulphur content.

Focussing on aspects of the fuel properties, sulphur and potassium contents likely play a key role in the formation of vehicular particles. For instance, the emission rate of particle number was found to decrease significantly (30-60%) by reducing the sulphur content in the diesel fuel from 500 to 5-50 ppm (Bagley et al., 1996; Jones et al., 2012; Kittelson et al., 2002; Ristovski et al., 2006). The PNSD is also substantially affected by fuel sulphur content (Jones et al., 2012; Wang et al., 2011b).

2.1.1.3 Effects of vehicle operating modes and particle after-treatment devices

The operating mode including the vehicle speed, acceleration and load were found not to have a significant influence on the size distribution, even though these had strong effects on the number and mass concentrations in both chassis and on-road measurements of a light-duty gasoline vehicle (Li et al., 2013). On the contrary, for particles emitted from a diesel engine, the particle size depends heavily upon the vehicle speed and load (Giechaskiel et al., 2005). For example, the number mode of particles generated from a heavy duty diesel engine was smaller than 25 nm at a speed of 1600 rev/min and from 40 to 60 nm at 2600 rev/min (Shi et al., 1999). In addition, the dilution conditions including the dilution system, dilution ratio, temperature and humidity, have a strong impact on the size of particles since these control the particle nucleation rate (Casati et al., 2007; Maricq et al., 2001; Shi and Harrison, 1999).

Particle control technologies such as oxidation catalysts and particle traps have also been developed and applied in recent years. The particle trap is one of the best ways to reduce soot and related black smoke emissions from vehicles with an efficiency of more than 99% found for particles (Mayer et

al., 2002). Giechaskiel et al. (2010) evaluated the efficiency of a volatile particle remover system. The results showed that 40-90% of the condensed material in the size range ~50-500 nm was removed and 99% of particle number in the nucleation mode was wholly evaporated or was decreased to sizes less than 23 nm.

2.1.2 Non-exhaust vehicular particle emission

Non-exhaust particles which typically arise from road-tyre interaction, brake wear, and re-suspension also contribute significantly to urban airborne concentrations.

2.1.2.1 Brake wear

The particles generated from the mechanical process of brake wear have a wide range of diameters from a few hundred nanometres to a few tens of micrometres (Thorpe and Harrison, 2008). The particle number distributions measured by optical methods in many studies show a bimodal or tri-modal size distribution with the peak around 300 nm. Mosleh et al. (2004) conducted a pin-on-disc test of brake wear particle emissions from a truck semi-metallic pad material against grey cast iron under different controlled contact pressure and sliding velocity and found a bimodal PNSD. They noted that all the measurements showed a similar first peak at 350 nm; however the second peak could vary from 2 μm to 15 μm and shifted to a larger size with higher loads. Using EDX analysis, they proposed that submicron particles, which mainly consist of iron, carbon and oxygen, are mainly generated from the cast iron disc, while larger particles originate from the brake pad material and contain aluminium, magnesium, antimony, silicon, sulphur, and copper. This study is in agreement with Wahlström et al. (2010b) who compared the particle sizes of airborne wear particles emitted from passenger car disc brakes from three test conditions including field tests, a disc brake assembly test stand, and a pin-on-disc machine test. They found that all tests showed a similar number size distribution with dominant peaks around 280 nm and 350 nm, with independence of different load conditions, sliding speed, and pad temperature. A further

comparison between the particle wear debris originated from the interaction of non-asbestos organic (NAO) and low-metallic pads with grey cast iron rotors showed that the number concentrations generated from NAO pads were lower than those from low-metallic pads, but the size distributions were similar.

Several studies have reported aerodynamic diameters and have noted a primary peak at approximately 1 μm. Iijima et al. (2007) found that the number size distribution displayed a peak mode of 1-2 μm and the mass size distributions show a peak in the range 3-6 μm using an TSI Aerodynamic Particle Sizer (APS). This peak mode (1-2 μm) was different to those (0.35 μm) measured by a GRIMM optical particle sizer. This difference could be explained by the different types of particle diameter due to differing measurement principles of different instruments. For example, the APS measures particle size based on the aerodynamic properties while the SMPS uses electrical mobility diameter and the GRIMM optical sizer uses light scattering. In addition, it is also noted that there are inherent instrument differences even when using the same physical principle, such as the difference between TSI SMPS and GRIMM SMPS (Jeong et al., 2009; Joshi et al., 2012; Kaminski et al., 2013). Wahlström et al. (2010b) used a particle density of 5 g/cm^3 from Sanders et al. (2003) to calculate the maximum peak size as an aerodynamic diameter from an optical diameter (0.35 μm) measured by GRIMM optical spectrometer. They found the peak size shifted from 0.35 μm optical diameter to 0.9 μm aerodynamic diameter, consistent with reports from Aerodynamic Particle Sizer measurements. Table 3 shows an overview of size distribution of brake wear particles.

Because of the inability of optical techniques to identify the ultrafine particles, which can comprise a significant proportion of brake emissions (Wåhlin et al., 2006), some recent studies have applied a Scanning Mobility Particle Sizer (SMPS) system to measure particle sizes from 10 nm to 600 nm. For example, Abbasi et al. (2012b) conducted a pin-on-disc test of the rate and size of airborne

particle emissions from railway braking materials. The disc samples were made from a wheel and a brake disc (steel), while the pins were made from brake pads (organic or sintered), and brake blocks (organic or cast iron). They found that there is one major peak around 70-120 nm partially in the ultrafine particle region and two minor peaks around 300-400 nm and 500-600 nm in the fine particle region, depending upon the type of discs and pins. These results are consistent with previous work by Olofsson (2011) and Wahlström et al. (2010a).

Garg et al. (2000) reported that particle counts (4.17×10^{12} particles/stop at 400^{o}C) measured using a TSI Electrical Aerosol Analyser (that measures all particles larger than 10 nm) were much higher than those (5.23×10^{6} particles/stop) measured by a Dekati electrical low-pressure impactor (ELPI- with stage cut points from 30 nm to 10 µm) when they conducted a brake dynamometer test under four wear conditions, which suggested that most particles are smaller than 30 nm. The evidence for nanoparticles formed from brake emissions was observed by using a Fast Mobility Particle Sizer (FMPS) and engine exhaust particle sizer (EEPS). Mathissen et al. (2011) set up a sampling tube close to the brake disc of a diesel car and measured the particle sizes under different driving situations using the EEPS. They found that the full braking presented a unimodal PNSD with a peak at approximately 11 nm. A similar result was found in a recent study by Kwak et al. (2014) who measured ultrafine particles from brake emissions using a proving ground and road simulator. The mechanism of nanoparticle formation from brake emissions is unclear. Sanders et al. (2003) suggested that due to very high temperatures during the brake wear process some of the brake pad and lining materials can volatilise and therefore form the small particles by condensation. Kwak et al. (2014) proposed that the thermo-oxidative degradation of organic materials or metals contained in brake linings could lead to nanoparticle formation.

2.1.2.2 Tyre- road surface interaction and resuspension

313 The interactions of tyre and road surface lead to the abrasion of the tyre tread and it has often been
314 assumed to form primarily coarse particles (> 2.5 µm) (Thorpe and Harrison, 2008). Dannis (1974)
315 reported that the mean diameter of tyre wear particles was in the range of 20 µm with few particles
316 below 3 µm found. However, not all tyre wear particles become airborne, just a small proportion,
317 due to settling on the road surface under gravity as such large particles have a short atmospheric
318 lifetime with respect to deposition (Thorpe and Harrison, 2008).
319
320 Interestingly, evidence for a significant contribution of ultrafine and fine particles from tyre wear
321 emissions has also been found. Fauser et al. (1999) reported that particles with a diameter smaller
322 than 1µm accounted for approximately 90% of total airborne particles from tyre wear emissions.
323 The volatilisation and re-condensation of tyre wear materials were suggested as the main processes
324 leading to small particle formation (Cadle and Williams, 1979). The evidence for ultrafine particles
325 has been supported by some recent laboratory experimental studies. Dahl et al. (2006) found that
326 the estimated number concentration of ultrafine particles (15-700 nm) from the pavement-tyre
327 interface was 2.5 x 10^4 cm^{-3}, which was 10 times higher than the background number concentration
328 (~1-2 x 10^3). The mean particle diameters were in the range of 15-50 nm which were similar to
329 particles emitted from light duty vehicle exhaust emissions. Likewise, Gustafsson et al. (2008)
330 reported that the estimated number concentrations of ultrafine particles (15-700 nm) from the
331 interaction between tyre, road pavement and winter traction sand ranged from 0.12 to 2.65 x 10^4
332 cm^{-3}, depending upon the type of road surface and vehicle speed. In terms of particle sizes, the
333 number size distributions showed a peak mode at 20-50 nm while the mass distributions revealed
334 two peak modes at 4-5 µm and 7-8 µm. In a further study conducted by Aatmeeyata et al. (2009),
335 tyre wear particles in the size range of 0.3- 10 µm showed a bimodal distribution with peaks at 0.3
336 and 1.7 µm in the number size distribution.
337

Resuspended dust contains particles originating from the resuspension of road surface deposited materials (i.e. debris of brake or tyre wear from vehicles, soil or crustal emission, de-icing salt and sand) by tyre shear and wind or traffic-induced turbulence (Kumar et al., 2013; Thorpe and Harrison, 2008; Thorpe et al., 2007). Lenschow et al. (2001) reported that the re-suspended road dust particles contributed 50% of the total roadside increment of PM_{10}. Similar results have been found in other studies conducted by Harrison et al. (2001) and Forsberg et al. (2005). There are limited studies of number particle size distributions and concentrations. Harrison et al. (1999) reported that these particles were distributed mainly in the coarse mode (2.5-10 μm) and showed a distinct seasonality with a summer maximum and winter minimum.

2.2 Industrial Combustion Emissions

Industry is one of the major contributors of air pollutants to urban areas. In industrial areas, the emissions from industrial combustion processes and traffic contribute mainly to the fine and ultrafine particle fractions. In this section, we aim to summarize the particle size distribution of emissions measured during coal fired combustion, oil combustion and municipal waste incineration. The particle number modes measured in different combustors and plants are shown in Table 4.

2.2.1 Coal combustion

Coal combustion generates particles with a size ranging from a few nanometres to millimetres. The small particles which are initially formed by vaporisation, nucleation, chemical reactions, and by growth due to coagulation and condensation processes contain predominantly condensed and semi-volatile materials, while the larger particles consist of mainly carbonaceous materials, fragments of inorganic fly ash and trace elements.

In the number count, the majority of particles are in the submicron mode. The median diameter varies between 30 and 80 nm, depending upon a number of factors, such as coal type, combustion

364 temperature, dilution ratio, residence time, treatment device and other sampling conditions
365 (Carbone et al., 2010; Li et al., 2009; Lighty et al., 2000; Linak and Peterson, 1984; Lipsky et al.,
366 2002; Lipsky et al., 2004). Suriyawong et al. (2006) measured the submicron particle number size
367 distribution from coal combustion in a typical O_2:CO_2 and air system and found a bimodal number
368 size distribution with a major peak around 30-54 nm and a minor peak at 300 nm. O_2:CO_2 and
369 O_2:N_2:CO_2 mixing ratios had strong effects not only upon the mass concentration but also the
370 number concentration and its size distribution. For example, the geometric mean diameter (GMD)
371 was observed to increase from 29 to 54 nm as the O_2:CO_2 ratio was changed from 0.25 to 1. In a
372 O_2:N_2:CO_2 system, as the ratio of N_2:CO_2 with fixed O_2 level increased, the GMD also increased
373 from 31.2 to 40.5 nm. This study concluded that different mixing ratios could change coal particle
374 surface temperature, affecting the vaporization rate, and resulting in the particle growth.
375
376 Electrostatic precipitators (ESP) are the most popular particle control device applied on coal power
377 plants. Collection efficiency is particle size-dependent, and hence the shape of the particle size
378 distribution is likely to change upon passage through the ESP (Li et al., 2009). Mohr et al. (1996)
379 reported that ESP particle control devices have lower collection efficiency in the size range between
380 200 and 400 nm and the measured number peak mode after ESP treatment was shifted to larger
381 sizes due to the penetration characteristics of the ESP. In an other study, Zhuang and Biswas (2001)
382 found that sorbent injection also increases the mean size of the coal combustion aerosol by
383 suppressing nucleation and promoting condensation on agglomerated sorbent particles.
384
385 A nucleation peak mode around 10 nm was found in the stack plume from coal combustion emitted
386 to ambient air (Lipsky et al., 2002; Wang et al., 2008). As with the exhaust emissions from internal
387 combustion engines, the presence of inorganic compounds could explain the nucleation of particles
388 from coal combustion. Lipsky et al. (2002) supposed that once entering a dilution tunnel, the coal
389 combustion emission is diluted and cooled, resulting in H_2SO_4 formation from the SO_3-H_2O

reaction. The rapid cooling of the coal emissions leads to a supersaturation of H_2SO_4, causing new particle formation due to nucleation. This study also reported that both nucleation and coagulation rates increase as the dilution ratio increases and noted that the ultrafine particle number concentrations increase and shift to smaller sizes. In addition, Wang et al. (2011a) found a reduction of around 50% in the number of ultrafine particles following the shutdown of a large local coal-fired power plant, although no distinction was made between primary emissions and secondary particles.

2.2.2 Oil combustion

Morawska et al. (2006) measured the particles emitted from an oil shale boiler in both the stack plume and at a sited located 4.5 km from the plant. The PNSD was similar at the two sampling sites, and showed a bimodal lognormal distribution with CMDs of 24-27 nm and 50-52 nm. Similar to other fuel combustion, the first mode was attributed to formation from nucleation and the second mode comprised primary particles consisting of carbonaceous compounds and condensed semi-volatile material. In an other study, Chang et al. (2004) compared the size distributions of particles measured in flue gas of a pilot-scale test combustor using coal, heavy fuel oil and natural gas. The CMD of the size distribution from heavy fuel oil combustion was around 70-100 nm, which is similar to diesel combustion at low dilution ratios (suppressing the nucleation mode) but was larger than from coal combustion (40-60 nm) and natural gas combustion (15-25 nm).

2.2.3 Waste incineration

There are several reports of particle size distributions measured in the flue gas and stack plume emitted from municipal waste incineration plants (Buonanno et al., 2009a; Cernuschi et al., 2012; Maguhn et al., 2003). Maguhn et al. (2003) measured particle sizes in both the flue gas and stack plume of a municipal waste incineration plant. At the 700^{o}C sampling point (grate exit, prior to the boiler), they showed a bimodal size distribution with a peak mode at approximately 90 nm and a

416 minor mode at about 40 nm. When sampled after the boiler (at 300^{o}C), the major peak mode shifted
417 to 140 nm and the minor peak mode observed at 700^{o}C disappeared, suggesting the growth of
418 particles by absorption and coagulation processes. Changes in combustion conditions such as the
419 operation of back-up oil burners or cleaning which influence the soot particles, the flue gas
420 composition and re-suspended mineral particles, can alter the measured particle size distribution.
421 Within stack plume measurements (at 80^{o}C), showed the peak mode reduced from 140 nm to 40-70
422 nm, which could be explained by the influence of the fabric filter and wet-ESP. The retention
423 efficiency of the fabric filter for particles of > 100 nm was found to be higher than those for
424 ultrafine particles (17-70 nm) and the efficiency of the wet-ESP is likely to be slightly poorer for
425 particles with a diameter smaller than 50 nm, therefore shifting the size distribution to smaller
426 particles. This is in agreement with Buonanno et al. (2011b). In addition, the particle removal
427 efficiency of the fabric filter was found very high (> 99.99 %) (Buonanno et al., 2011a; Buonanno
428 et al., 2011b). As a result, the consensus from studies of European waste incinerators is that particle
429 concentrations in stack emissions are comparable with, or lower than, those typical of ambient air,
430 and hence no source signature is visible in ground-level atmospheric measurements (Buonanno and
431 Morawska, 2015; Buonanno et al., 2011b; Ozgen et al., 2012).
432
433 **2.3 Biomass Burning**
434 Freshly generated smoke particles from biomass combustion consist mostly of organic carbon with
435 ~10-20% black carbon and inorganic species and are found predominantly in the accumulation
436 mode. The particle size distributions vary depending on combustion appliance, fuel type,
437 combustion phase and sampling method.
438
439 On a laboratory-scale, Wardoyo et al. (2006) reported that particle sizes initially showed a unimodal
440 distribution with a CMD of 50-70 nm, and 30-40 nm during the flaming and smouldering phase
441 from fast burning of wood. The CMD was found to be larger in a slow burning process with CMDs

of 110-150, 50-60 and 30-40 nm during the ignition, flaming and smouldering phases. This study was consistent with Hosseini et al. (2010), who reported that particle size showed uni- or bimodal distributions with a major mode ranging from 29 to 52 nm. In terms of type of fuels, Chakrabarty et al. (2006) reported that burning wet fuels (tundra core and Montana grass) produced large particles with CMD of 120-140 nm, compared to small particles with CMD of 30-70 nm from burning dry fuels.

In field experiments, most studies have shown a consistent size distribution, with the count median diameter of 100-160 nm for fresh smoke (Reid et al., 2005). Janhäll et al. (2010) calculated the averaged count mean diameter and geometric standard deviation of fresh smoke to be 117 nm and 1.7 from 20 datasets from previous publications (Guyon et al., 2005; Reid and Hobbs, 1998; Reid et al., 1998). During the ageing process, particles can increase their median diameter up to 235 nm by coagulation/condensation (Janhäll et al., 2010).

2.4 Cooking Emission

Cooking emissions are a major source of submicron particles in indoor environments (Abdullahi et al., 2013). Wallace (2006) found that aerosol concentrations generated during only 15 minutes of cooking increase by a factor of 14, approximately 90% of which were found predominantly in the ultrafine range in a house. Cooking aerosol can contribute significantly to ambient air concentrations; Harrison et al. (2011) found that cooking made a significant contribution (nearly 7%) to particle number at a major kerbside site in London.

The particle size distribution from cooking activities has been reported as unimodal with a peak generally between 20-70 nm, depending on the food type, heat source and cooking temperature as

466 shown in Table 5. Some studies, however, have reported peaks in the range 100-160 nm (Hussein et
467 al., 2006a; Yeung and To, 2008b).
468
469 Li et al. (1993) reported the particle size from three typical cooking process including scrambling
470 eggs, frying chicken, and boiling soup and found that the particle modes were 40 nm, 50 nm and 30
471 nm diameter, respectively. Similarly, Buonanno et al. (2009c) found that a higher concentration of
472 particles was generated by cooking fatty foods and the number mode diameters for fatty foods
473 (cheese, wurstel, bacon) were between 40 and 50 nm while those for vegetable foodstuffs
474 (eggplants) were around 30 nm.
475
476 In a comparison of heat sources, Dennekamp et al. (2001) found a higher particle number emitted
477 by a gas grill compared with using an electric grill or a gas or electric ring hob. Particles emitted
478 from gas stoves were in the size range 15-40 nm, while those generated from fried bacon by gas or
479 electric rings have a larger diameter (50-100 nm). This is consistent with the results reported by
480 Buonanno et al. (2009c). He et al. (2004) reported that the particle size and emission factor for
481 cooking aerosol also depend upon stove properties such as stove temperature. The reader is referred
482 to the work by Abdullahi et al., (2013) for a comprehensive review of particle number size
483 distributions associated with cooking emissions.
484
485 **2.5 Long Range Transported Aerosols**
486 Long-range transported aerosols comprise mostly accumulation mode particles, with the major
487 number peak mode around 100-200 nm. Aitken and nucleation mode particles have short lifetimes
488 due to their rapid coagulation and condensational growth, and coarse mode particles are removed
489 relatively rapidly by gravitational settling, whereas particles in the accumulation mode can be
490 transported over long distances because they are too small to deposit by inertial and gravitational
491 processes and too large to be influenced appreciably by growth processes (Hussein et al., 2006b).

Accumulation mode particles are most significantly removed from the atmosphere by precipitation scavenging (Seinfeld and Pandis, 1998). During long-range transport of air masses SO_2 can oxidise leading to nucleation and then growth, hence sometimes long-range transported air also contains nucleation and Aitken mode particles (Wang et al., 2011a,b).

Accumulation mode particles can be generated directly from combustion processes such as wood burning or traffic emissions, or from the growth of smaller particles such as Aitken mode particles by coagulation and condensation during transportation. In a clean environment, such as the background free troposphere or remote marine boundary layer, these particles are influenced largely by cloud processing (Hoppel et al., 1994a,b).

The particle size distributions of long-range transported aerosols have been observed clearly in remote or urban background areas. Raes et al. (1997) observed particle size distributions at the Global Atmospheric Watch Observatory on the mountain of Izaña (IZO), at 2360 asl on the island of Tenerife. This study found that the PNSD showed a dominant unimodal structure with a GMD of 120 nm and 55 nm during dusty and clean conditions respectively. These accumulation mode particles were attributed to desert dust in the size range of 100-200 nm transported from northern Africa or aged anthropogenic sulphate transported from southern Europe.

Similarly, Sellegri et al. (2010) observed the seasonal variations of PNSD at a high altitude Himalayan site (5079 m) and found higher particle number concentrations due to the increase of accumulation mode particles in the late afternoon during the pre-monsoons. The increase of these accumulation particles was accompanied by an increase of black carbon and coarse mode particles. This study concluded that these particles are evidence of the transport of regional or long-range polluted aerosols. Similar results have been reported by Gogoi et al. (2014) and Adak et al. (2014).

2.6 Marine Aerosols

In general, marine aerosol can be divided into two broad categories: (1) primary sea-salt aerosol formed by the mechanical disruption of the ocean surface and (2) secondary aerosol predominantly contributed by non-sea salt sulphate and organic species due to gas-to-particle conversion processes (O'Dowd et al., 1997). The total particle number concentration of marine aerosol ranged from 200 to 800 cm^{-3}, depending on the regional latitudes but there was no significant interhemispheric difference (Heintzenberg et al., 2000). Koponen et al. (2002) reported that the total particle concentrations were predominantly lower than 1000 cm^{-3} measured in marine air masses.

The typical marine particle number spectra show two modes: an Aitken mode with a mean diameter around 40-52 nm and accumulation mode with a mean diameter of around 150-175 nm. In some studies, a nucleation mode was also present with two distinct peaks: one around 10 nm and another in the range of 15-20 nm (Koponen et al., 2002). A sea salt mode with a mean diameter above 400 nm is frequently found in the marine boundary layer (Heintzenberg et al., 2000). Fine particles contributed 90-95% of the total particle number while the mass distribution showed two distinct modes, one fine and one coarse. The coarse mode only accounted for 5-10% of the total number of particles, but contributed 90-95% of total mass (Fitzgerald, 1991).

2.7 Nucleation

New particles formed by nucleation account for a significant fraction of the total number of particles in the atmospheric environment. A review of the formation and growth of ultrafine particles conducted by Kulmala et al. (2004) found that nucleation events occurred in both clean and polluted environments: the continental boundary layer, remote boreal forest, suburban, rural, industrialised agricultural regions or coastal environments. The high frequency occurrence of nucleation events has also been observed in some urban environments in many studies (Dunn et al., 2004; Reche et al., 2011). A study conducted by Gao et al. (2012) found that new particles formed

by homogeneous nucleation occurred on 42.7% of days in a two-month study period in Beijing (China), while the frequency of nucleation events observed in Pittsburgh (US) was about 50% of days (Stanier et al., 2004b). A high frequency of nucleation events was found in other cities such as Brisbane (Australia), Rochester (US) and Beijing (China) (Cheung et al., 2011; Jeong et al., 2004; Wehner et al., 2004). A very much lower frequency was reported in Birmingham (UK) by Alam et al. (2003).

Nucleation events are characterised by a rapid increase of particle number concentration in the nucleation mode causing the peak mode to shift to small particle diameters. Stanier et al. (2004b) found the number concentration of particles during weak nucleation events and that in relatively intense events ranged from $5x10^4$ cm^{-3} up to $1.5x10^5$ cm^{-3}. Similar results observed in Beijing by Wehner et al. (2004) also showed that the number concentrations of particles increased 10 times from 10^4 to 10^5 cm^{-3} during nucleation events. Jeong et al. (2004) observed two types of nucleation event in Rochester. The first type with a dominant particle size ranging from 20 to 100 nm was found typically during the morning rush hour (07:00-09:00) and often in the late afternoon rush hour. These nucleation events were attributed to the new particle formation from local plumes, and particularly traffic emissions as discussed in Section 2.1.1 above. The second type of nucleation events were observed during the afternoon with a peak at around 13:00 and had a particle size range of 11-30 nm. Stanier at al. (2004b) described atmospheric nucleation events as two groups, namely "short-lived" and "regional" events. In the "short-lived" group, there was a rapid increase of number particle in the nucleation size range, but nuclei particles did not grow to larger particles. Jeong et al. (2006) found this "short-lived" nucleation events related to local SO_2 and solar radiation (UV-B), indicating that the photochemical reaction of SO_2 and OH radicals produced from O_3 photolysis could be responsible for this type of nucleation event. In the "regional nucleation" event, new particles can grow up to 100 nm over several hours in the late afternoon and evening (the PNSD evolution can be seen in the so-called banana curves). Similarly, Cheung et al. (2011)

570 observed three cases of nucleation burst events which were classified as: (i) new particle formation
571 by photochemical processes; (ii) a nucleation burst without particle growth and (iii) the interplay
572 between these two cases. In the first case with photochemically driven nucleation, the GMD
573 reached the smallest value of the day (~ 8 nm) during the nucleation occurrence period, and then the
574 nucleation mode particles grew into larger particles (~ 57 nm) until around midnight. In the second
575 case of a nucleation burst occurring without growth into larger particles, the GMD dropped from
576 ~30 nm to 10 nm and the number of particles in the nucleation mode increased from ~7.10^3 to 10^5
577 cm^{-3} while those in the Aitken mode did not show any significant variation (Cheung et al., 2011). It
578 was suggested that the nucleation burst could be due to the nucleation of local precursors emitted
579 from local sources such as traffic, ship or aircraft emissions. Reche et al. (2011) demonstrated the
580 frequent occurrence of particle nucleation between the morning and evening rush hour periods in
581 southern, but not northern European cities, and Brines et al. (2015) distinguished between traffic
582 and nucleation events as sources of nanoparticles in high insolation developed world cities,
583 following a quantitative estimation of source contributions conducted in Barcelona (Dall'Osto et al.,
584 2012). In later work, Dall'Osto et al. (2013) distinguished three types of nucleation and growth
585 events: (1) a regional type event affecting both the city and the surrounding rural area; (2) a
586 regional event impacting only the surrounding rural area, and (3) an event originating in the city and
587 continuing downwind. For criteria to identify nucleation events, the reader is directed to other
588 sources (Kulmala et al., 2012; Betha et al.,2013; Dal Maso et al., 2005; Manninen et al., 2010; Woo
589 et al., 2001; Wu et al., 2007).
590
591 Reche et al. (2011) compared diurnal profiles of particle number count and black carbon in a
592 number of European cities. In northern Europe, particle number generally correlated strongly with
593 black carbon reflecting a common source in road traffic emissions. In the data from southern
594 European cities an additional increase in particle number count, not associated with black carbon
595 occurred in the middle of the day, and was attributed to regional nucleation processes driven by

photochemistry (Reche et al., 2011). The seasonal occurrence of nucleation has been found to vary. Stanier et al. (2004b) found that regional nucleation events occurred during all seasons but the most intense ones were observed during spring and fall. Jeong et al. (2004) reported that there was no clear seasonal variation of the afternoon nucleation occurrence frequency. However, that study noted that strong afternoon events with number concentrations of particles higher than 30,000 cm^{-3} were mostly found in spring and summer.

The mechanisms for new particle formation have also received much attention from researchers. There are two mechanisms that explain the nucleation of particles in the atmosphere: (1) condensation of a low-vapour-pressure species without foreign nuclei or surface involved (homogeneous nucleation) or (2) scavenging of the low-vapour-pressure products on a foreign substance (heterogeneous nucleation). Holmes (2007) expressed the view that most secondary particles formed within the atmosphere possibly occur by binary nucleation of sulphuric acid and water or ternary nucleation involving a third molecule which is frequently ammonia. Furthermore, Zhang et al. (2011) presented a critical review of nucleation and growth of nanoparticles in the atmosphere. That review concluded that the binary nucleation or ternary nucleation of sulphuric acid, water and ammonia cannot explain completely the observed nucleation frequency and growth rate, suggesting that other nucleation mechanisms (i.e. ternary nucleation of H_2SO_4-H_2O involving amines, nucleation of iodine oxides or ion-induced nucleation) could participate in new particle formation. For more information on nucleation process mechanisms, the reader is directed to other sources (Holmes, 2007; Pitts and Pitts, 2000; Seinfeld and Pandis, 1998).

3. FACTORS AFFECTING PARTICLE NUMBER SIZE DISTRIBUTIONS

As discussed above, particles emitted from different sources show different size distributions, and therefore the shape of a measured PNSD in the atmosphere depends upon the contributing sources and atmospheric processing between source and receptor for both primary and secondary aerosols.

622 The evolution of PNSD from traffic exhaust emissions to ambient air has been investigated by
623 numerous experiments especially in traffic tunnels, street canyons or freeways which show a change
624 in PNSD with increasing distance from local emissions (Agus et al., 2007; Hitchins et al., 2000;
625 Zhu et al., 2002b). For example, Zhu et al. (2002b) reported that the ultrafine particle size
626 distribution changes significantly with increasing distance from a freeway. The study reported that
627 the PNSD shows three distinct modes with GMD of 12, 27 and 65 nm at 30 m downwind distance;
628 while it shows one mode with GMD of 41 nm at 150 m downwind and two modes with GMD of 15
629 and 65 nm at 300 m downwind. By conducting experiments of the evolution of PNSD near the 405
630 and 710 freeways in Los Angeles, California, Zhang and Wexler (2004) concluded that PNSD alters
631 due to nucleation, condensation and coagulation in the very rapid first-stage dilution process (1-3 s)
632 which is induced by vehicle turbulence. In the second dilution process which can last around 3-10
633 min, the main mechanisms in changing the particle number size are condensation, evaporation and
634 dilution while the effects of coagulation and deposition are minor (Zhang et al., 2004; Jacobson and
635 Seinfeld, 2004). As a result, Zhang et al., (2004b) found that a dominant fractions of particle
636 number grew into the size range of > 10 nm at around 30-90 m downwind distance while some of
637 them continued to grow to >100 nm and some shrank to <10 nm beyond 90 m of the freeways.
638 Similar findings were observed in a study on the impact of roadside noise barriers on PNSD near
639 freeways by Ning et al. (2010). Dall'Osto et al. (2011a) reported that traffic-generated
640 nanoparticles shrank by evaporation as they were carried downwind into a park, or mixed upwards
641 within the atmosphere. In a review of dynamics and dispersion modelling of nanoparticles from
642 roadside sites, Kumar et al. (2011) concluded that dilution is the most essential input parameter in
643 dispersion models, followed by the nucleation, condensation and deposition. Obviously,
644 meteorological parameters such as wind speed, wind direction, temperature and humidity have
645 significant roles in altering PNSD due to their strong effects in the dilution, nucleation,
646 condensation and evaporation of particles (Birmili et al., 2001; Charron and Harrison., 2003; Nieto
647 et al., 1994; Vakeva et al., 2000). For example, Shi and Harrison (1999) found that nucleation of

particles during diesel exhaust dilution was favoured by high relative humidity and low temperatures. Similarly, Ketzel et al., (2007) found that the particle number emissions can double due to a higher nucleation rate by a decrease of temperature from 20 to 5^{o}C. In addition, Charron and Harrison (2003) observed the evolution of PNSD at a major road in London and found that wind and rain have a strong influence on the particle number. This study found the stronger wind speed could reduce twofold total number counts of particles at diameter ranging from 30 to 450 nm, but had no effect on the small particles (11-30 nm), and particle numbers with diameter below 150 nm were found higher during the rainy periods. In an other observation in a Northern Indian City, Baxla et al. (2009) found that the particle number concentration on a winter foggy day was an order of magnitude higher than a winter clear day and the particle size distribution show a high number of ultrafine particles less than 20 nm. The higher number concentrations observed on foggy days could be explained by the enhanced secondary organic aerosol production due to aqueous phase chemistry during these episodes (Kaul et al., 2011). Furthermore, the other properties of particles such as hygroscopicity can play a significant role in changing particle size (Swietlicki et al., 2008; Weingartner et al., 1997; Rose et al., 2010).

During transportation in the atmosphere, both primary and secondary particles continue to be subject to the processes of growth (coagulation, condensation, evaporation and cloud nuclei formation) and removal (dilution, settling, deposition, rainout, and washout) (Hinds, 1999). Hence, number concentration and diameter of particles can change during transport. The influences of atmospheric processes on particles vary depending on their size. For example, nuclei mode particles are strongly affected by coagulation due to their frequently high number concentration. The influence of atmospheric processes can be observed via studies on ageing of combustion particles in both the laboratory and the field. Interestingly, the influence of atmospheric processes has been explained well in recent studies by application of receptor models on measured PNSD, as will be discussed in detail in the following section.

4. APPLICATION OF PNSD IN SOURCE IDENTIFICATION AND APPORTIONMENT

4.1 Modal Analysis Methods

The PNSD is ideally described by the log-normal distribution. For a unimodal distribution, a $\log_{10}$-normal distribution function is described by equation (1) (Pitts and Pitts, 2000):

$$\frac{dN}{dlogD_p} = \frac{N}{\sqrt{2\pi}log\sigma_g}\exp[\frac{-(logD_p - logCMD)^2}{2(log\sigma_g)^2}] \quad (1)$$

where:

N: total number concentration and dN is the particle number concentration having a logarithmic diameter between logDp and (logDp+dlogDp) (cm^{-3}); D_p: particle diameter (nm); σ_g: geometric standard deviation; CMD: Count median diameter (nm).

As discussed in the above sections, measured PNSDs in the atmosphere typically have more than one mode. Therefore, they can be considered as a sum of *n* modes that fit a sum of lognormal distributions, in which each mode reflects a different source as described in Equation 2.

$$\frac{dN_{Total}}{dlogD_p} = \frac{dN_1}{dlogD_p} + \frac{dN_2}{dlogD_p} + \cdots + \frac{dN_n}{dlogD_p} \quad (2)$$

Mäkelä et al. (2000) applied a fitting procedure to one year of submicron particle data from a tropospheric background site in Southern Finland. This study found that there were three typical modes including the nucleation mode, the Aitken mode and the accumulation mode. They sometimes found a fourth and a fifth mode. Similarly, by analysis of modal parameters at an urban roadside location, Lingard et al. (2006) found four modes including mode I - sub-11 nm nucleation mode (CMD: 7-11 nm, σ_g: 1.1-1.4), mode II- super-11 nm nucleation mode (CMD: 11-25 nm, σ_g:

1.3-1.6), mode III-Aiken mode (CMD: 28-86 nm, σ_g: 1.5-2.0) and mode IV- accumulation mode (CMD: 114-173 nm, σ_g: 1.2-1.5). Mode-I was interpreted as arising from atmospheric nucleation or oxidation of post-exhaust emissions from vehicles. Mode II was particles that shared some common sources with mode-I particles, whilst they were also believed to come from photolysis driven sources and condensation of the vehicular emissions. However Mode II was believed to also represent new particle formation "through aged air masses rich in precursor gases from anthropogenic sources" at the beginning of the day. Mode III particles were interpreted as externally mixed soot particles which were primarily generated from diesel engines while mode IV particles were attributed to secondary aerosols which formed in the atmosphere by coagulation and agglomeration of small particles or condensation of volatile materials onto pre-existing particles. These results are consistent with Agus et al. (2007).

4.2 Cluster Analysis

The application of clustering techniques to size distribution data was first performed by Tunved et al. (2004). Subsequently, it has been used by numerous recent studies (Beddows et al., 2014; Beddows et al., 2009; Brines et al., 2014; Charron et al., 2008; Dall'Osto et al., 2011b; Wegner et al., 2012). In this method, the measured PSND spectra in a large dataset can be classified into controllable subgroups based on the highest degree of similarity between each PNSD spectrum. The clustering algorithm used, known as K-Means, selects a random initial partition and repeatedly assigns PSND spectra to categories by minimizing the sum of squared Euclidean distances between each spectrum and its cluster centre. In the initial result, a higher number of clusters around 10-20 is selected to avoid any possible combined PSND spectra from different sources or processes (Brines et al., 2014). To optimise the selected cluster number, use of the Dunn-Index -defined as a function of the ratio between cluster separation (minimum distance between SMPS spectra of neighbouring clusters) to the maximum cluster diameter (maximum separation of the SMPS spectra within the cluster)- was introduced by Beddows et al. (2009).

721 Tunved et al. (2004) used clustering on SMPS data collected at the Swedish continental background
722 station Aspvreten. By averaging of six consecutive hours, hourly SMPS data were reduced to four
723 distributions each day (00:00-06:00; 06:00-12:00; 12:00-18:00 and 18:00-24:00). Based on
724 clustering, these size distributions were classified into eight groups which represented three
725 different stages of the particle life cycle including fresh, intermediate and aged stages. Beddows et
726 al. (2014) used cluster analysis of hourly/daily/weekly SMPS data collected at 24 background sites
727 across Europe in 2008-2009. By investigation of nine clusters, this study successfully described the
728 atmospheric processes influencing aerosol life. Following particle size distributions as air masses
729 traversed trajectories across Europe, aerosol growth processes could be quantified (Beddows et al.,
730 2014). By combining with auxiliary data such as meteorological parameters and air pollutants
731 (PM_{10}, $PM_{2.5}$, O_3, NO_x, SO_2), the sources of particles can be successfully identified (Beddows et al.,
732 2009; Charron et al., 2008).
733
734 **4.3 Receptor Model Studies**
735 The characteristic profiles of particle size distributions from local sources suggest that particle size
736 data may probably be useful to identify and apportion the sources of aerosols using receptor
737 modelling methods (Zhu et al., 2002b). Many recent publications that used factor analytical
738 techniques to PNSD data in recent years have demonstrated that this method can successfully
739 apportion sources of particles (Viana et al., 2008). The advantages of this method are that it can
740 identify specific sources of very small particles, such as nucleation, and it can separate sources of
741 particles such as brake and tyre-wear. For example, using this method Ogulei et al. (2007) identified
742 two types of nucleation sources of sub-micron particles in Rochester, New York, which could not
743 be identified if receptor models were applied to chemical species data. However, this method has
744 some disadvantages associated with variable profiles of PNSD due to weather conditions. Ogulei et
745 al. (2007) reported that the seasonal variation of ambient temperature and solar intensity could lead
746 to unstable size distributions of particles, which made impossible to resolve the source profiles.

One of the main receptor models which has been used is principal component analysis (PCA). Chan and Mozurkewich (2007) performed absolute principal components analysis (APCA) in Southern Ontario and reported that APCA can be applied effectively to a dataset composed of PNSD data and originally measured particulate matter and gaseous pollutant data. Similarly, Costabile et al. (2009) applied principal component analysis to the PNSD in Leipzig city and found that several of the resulting factors could be associated with particle modes that represented specific sources of particles. Furthermore, by using PCA combined with multi-linear regression analysis on the dataset including PNSD, meteorological parameters, gaseous pollutants and chemical speciation of fine particles, Pey et al. (2009) and Cusack et al. (2013) apportioned sources of particles with diameters in the range of 13-800 nm and submicron particles collected at an urban background site in Barcelona.

The receptor modelling technique applied most to PNSD data is positive matrix factorization (PMF), which will be discussed in detail in the next section. The first study using PMF on PNSD was conducted by Kim et al. (2003) and successfully identified sources of particles including wood burning, secondary aerosol, diesel and motor vehicle emission in Seattle (US). Since then, numerous studies have apportioned source of particles in urban areas using PMF applied to PNSD. In comparison with other receptor models applied to PNSD, the PMF model is reported to run well. Kim et al. (2003) compared PMF and Unmix models in a study of the volume size distribution and its pattern at a centrally located urban site in Seattle and found that both PMF and Unmix show four similar factors. A recent comparison of PMF with PCA-APCA conducted by Friend et al. (2013), reported that PMF identified six sources whereas PCA-APCA resolved ten sources. Interestingly the six sources resolved by PMF were similar to those by PCA-APCA.

4.3.1 PMF application to PNSD

As mentioned above, PMF is the model most frequently applied to PNSD. Positive Matrix Factorization (PMF) is a widely used tool to identify and apportion the sources of particulate matter (PM) by analysing the measurement of observed species at the receptor site (Viana et al., 2008). In the source apportionment of PM mass, many chemical components contained in PM such as organic and black carbon, ionic species and heavy metals are typically included in the dataset run with PMF. Additionally, other observations such as PAHs, gaseous species, meteorological parameters, and traffic flow are also used to identify more sources.

In the source apportionment of particles in terms of number, each size bin in the dataset is considered as an input variable. The number of variables has ranged from 16 to 158, depending on the numbers of samples, the quality of variables and the goals of study. To smooth the size distribution data and reduce the uncertainty in the number concentration, some studies have tried to reduce the original number of size bins by summing sets of consecutive size bins (Thimmaiah et al., 2009; Zhou et al., 2005b). In addition, Zhou et al. (2004) suggested that data from the days with intense nucleation events that considerably affect the stability of particle size distribution data should be excluded. In addition, in some instances the last size interval has not been included because of the collection efficiency drop or low data capture (Gu et al., 2011; Kim et al., 2003). In some studies, auxiliary data such as ion species, heavy metals, gaseous pollutants, meteorological parameters and traffic data have been added to help separate and identify the sources of particulate matter (Harrison et al., 2011; Ogulei et al., 2006b; Thimmaiah et al., 2009). Table 6 shows published studies that have applied PMF to PNSD data.

4.3.2 Sampling instruments

Full range particle size distributions have mainly been measured using a Scanning Mobility Particle Sizer (SMPS) and Aerodynamic Particle Size Spectrometer (APS), capable of covering the range

from 3 nm to 18 μm with time resolution less than one hour. Other measurement systems which have been used are Differential Mobility Particle Sizer (DMPS) and twin differential mobility particle sizer (TDMPS) (Thimmaiah et al., 2009; Wang et al., 2013; Yue et al., 2008). As discussed previously, many studies have conclusively shown that the fine particles account for the majority of the particle number concentration, therefore more than 50% of studies have applied PMF to identify sources of ultrafine and fine particles. In long-term measurements, datasets were sometimes subdivided into individual seasons to avoid the experimental uncertainty resulting from to large season-to-season variability in ambient temperature and solar radiation intensity that would lead to unstable/non-stationary size distributions (Wang et al., 2013). Missing data has been generally replaced by the average concentration of particle in the same size bins with the uncertainties assumed as 3 times the mean (Gu et al., 2011; Ogulei et al., 2006b) and outlier data has been generally been replaced by the mean concentration of the preceding and subsequent sample value (Thimmaiah et al., 2009). Merging the data to accommodate differences between electrical mobility and aerodynamic diameters is necessary prior to application of PMF (Beddows et al., 2010).

4.3.3 Calculation of measurement errors and uncertainties

Since the error matrix for number particle counts is not provided by the experimental instruments, several methods to assign measurement errors (σ) have been reported. The most popular formula to calculate the measurement errors was introduced by (Ogulei et al., 2006a) as the following empirical equation (Equation 3):

$$\sigma_{i,j} = \begin{cases} \alpha(N_{i,j} + \bar{N}_j) & \text{if } N_{i,j} > 0 \\ 2\,\bar{N}_j & \text{if } N_{i,j} = 0 \end{cases} \quad (3)$$

where $\sigma_{i,j}$ is the calculated measurement error for size bin j and sample i. $N_{i,j}$ is the measured number concentration for size bin j and sample i, and $\bar{N}_j$ is the arithmetic mean of the reported values for size bin j. $\alpha = 0.01$ is an arbitrary constant and was determined by a trial and error method. The missing data are replaced by $\bar{N}j$, the mean value for the size bin, and the uncertainties are assumed to be three times $\bar{N}j$.

Another method was presented by Zhou et al. (2004), which calculated the measurement error for the size range between 3 and 22 nm (particles measured by the nano-SMPS) based on the estimated instrumental error (U) in each size bin, as shown in Equation 4:

$$\sigma_{i,j} = \left(\sqrt{\frac{N_{i,j}}{U_j}} + 1\right) \times U_j, \quad j=1,2,..,55. \tag{4}$$

where $\sigma_{i,j}$ is the measurement error, $N_{i,j}$ is the measured number concentration for size bin *j* and sample *i*, U_j is the instrumental error calculated to be the lower of the minimum nonzero values and the minimum difference of the concentration values within the size bin *j*. To reduce the error caused by the discontinuity between instruments, this study combined every consecutive five size bins (*j*) into a new single size bin (*h*). The measurement error for the combined size fraction distribution $N_{i,h}$ was calculated according to Equation 5:

$$D_p \leq 0.022\ \mu m, \quad \sigma_{i,h} = \frac{1}{5} \sum_{j=5h-4}^{j=5h} \sigma_{i,j} \qquad h=1,2,...,11 \tag{5}$$

With particles of $D_p > 0.022$ μm, this study suggested that the concentration differences between neighbouring size intervals are not significant, i.e. that the concentration of the five consecutive bins can be considered as five measurements of one size bin. Therefore, the measurement error can be described according to Equation 6:

$$D_p > 0.022\ \mu m,\ \sigma_{i,h} = [\max(x_{i,5h-4}, ...,x_{i,5h}) - \min(x_{i,5h-4}, ...,x_{i,5h})]\ /\ 2, \quad (6)$$

$$h=12,13,..,33.$$

842

843 A recent publication by Wang et al. (2013) reported that the aerosol flow rate, the counting
844 efficiency of the DMA and CPC, along with the diffusion loss correction are error sources in the
845 measurement of particle size distribution using a TDMPS. This study estimated that the error
846 fraction for small particles (<25 nm) and large particle were 15% and 10%, respectively.

847

848 In terms of the uncertainties required to input into PMF, the uncertainty matrix is computed using
849 known concentrations, measurement errors and detection limit values. Readers are referred to
850 Hopke (2003) and Paatero and Tapper (1994) for different ways of estimating uncertainties. In
851 addition, Table 7 shows several formulae to estimate uncertainty used in studies of particle number
852 concentration.

853

854 **4.3.4 Solution interpretation**

855 PMF solutions are interpreted based on (1) modal characteristics of number (volume) size
856 distribution, (2) diurnal patterns of contribution, (3) source contributions to total number or volume
857 concentration, (4) the correlation of G-matrix with the measured gaseous or composition species
858 and (5) source directionality by the local wind trajectories and conditional probability functions
859 (Ogulei et al., 2007). In addition, many studies combine PMF results with auxiliary information to
860 link source types with factor profiles. While the local wind trajectories and conditional probability
861 functions are used to identify the location of the sources that originated the emissions corresponding
862 with each factor; the correlation of the G matrix (source contributions) with auxiliary information
863 such as gaseous and chemical composition data contributes towards the identification of the nature
864 of the sources. A comparison of PMF applied to particle size distribution and chemical composition
865 data conducted by Gu et al. (2011) showed moderate to strong correlations between four factors

including resuspended dust, stationary combustion, aged traffic and secondary aerosol obtained from PNSD and chemical composition data. In addition, the outcomes of PMF are more successful in analyses performed with datasets that combine particle number size fraction distribution with gaseous data and chemical composition data (Kasumba et al., 2009; Ogulei et al., 2006b; Thimmaiah et al., 2009; Yue et al., 2008; Zhou et al., 2005a). Furthermore, by applying PMF to the combined data of size distribution with meteorological and traffic volume, Harrison et al. (2011) identified and separated specifically the components of on-road emissions, including tyre and brake wear. The factor profiles and their fingerprints are summarized in Table 8.

4.4 Source Apportionment of Particle Number in Urban Areas

Traffic related emissions have been found to be a major source of urban particles (Morawska et al., 2008). Gu et al. (2011) found that fresh and aged traffic emissions accounted for 25% and 40% of total particles in central Augsburg, Germany. An application of PMF to PNSD data in Erfurt reported that local traffic and remote traffic represented 78% and 15% of total ultrafine particles (0.01-0.10 μm) respectively.

The second major source of particles in an urban area is nucleation. Ogulei et al. (2007) and Kasumba et al. (2009) reported that nucleation from traffic emissions represented between 15% to 21% of total particles in Rochester. Ogulei et al. (2007) concluded that the most important sources in urban Rochester, New York were traffic, nucleation and industrial emissions accounting for more than 81% of total submicron particles. Other dominant sources found in urban areas were industrial emissions, secondary aerosol and residential heating. Table 9 shows a summary of particle number source apportionment in different cities over the world extracted from receptor model analysis.

5. CONCLUSION

In summary, most atmospheric particle size distributions generated from multiple sources can be described as a sum of log-normal distributions, and each source displays a characteristic modal structure such as peak mode or count median diameter. After emission from the source, particles are subject to various dynamic processes such as nucleation, coagulation or condensation that alter their sizes. By number, nanoparticles account for the majority of particles emitted from combustion sources and are the main contributors to particle number concentration in urban areas. Modal, cluster and positive matrix factorization analysis of PNSD can help to identify the sources of particles measured at a particular receptor site. Moreover, the influence of atmospheric processes can also be resolved using these methods. Furthermore, PMF model results consistently identify traffic emissions as a major source of particle number concentration in cities.

ACKNOWLEDGEMENT

This research is supported by European Community through FP7 MC-ITN 315760, HEXACOMM, Proposal No. 315760.

REFERENCES

Aarnio, P., Yli-Tuomi, T., Kousa, A., Mäkelä, T., Hirsikko, A., Hämeri, K., Räisänen, M., Hillamo, R., Koskentalo, T., Jantunen, M., 2005. The concentrations and composition of and exposure to fine particles (PM2.5) in the Helsinki subway system. Atmospheric Environment 39, 5059-5066.

Aatmeeyata, Kaul, D.S., Sharma, M., 2009. Traffic generated non-exhaust particulate emissions from concrete pavement: A mass and particle size study for two-wheelers and small cars. Atmospheric Environment 43, 5691-5697.

Abbasi, S., Jansson, A., Olander, L., Olofsson, U., Sellgren, U., 2012a. A pin-on-disc study of the rate of airborne wear particle emissions from railway braking materials. Wear 284, 18-29.

Abbasi, S., Olander, L., Larsson, C., Olofsson, U., Jansson, A., Sellgren, U., 2012b. A field test study of airborne wear particles from a running regional train. Proceedings of the Institution of Mechanical Engineers, Part F: Journal of Rail and Rapid Transit 226, 95-109.

Abdullahi, K.L., Delgado-Saborit, J.M., Harrison, R.M., 2013. Emissions and indoor concentrations of particulate matter and its specific chemical components from cooking: A review. Atmospheric Environment 71, 260-294.

Abt, E., Suh, H.H., Allen, G., Koutrakis, P., 2000. Characterization of indoor particle sources: A study conducted in the metropolitan Boston area. Environmental Health Perspectives 108, 35.

Adak, A., Chatterjee, A., Singh, A.K., Sarkar, C., Ghosh, S., Raha, S., 2014. Atmospheric Fine Mode Particulates at Eastern Himalaya, India: Role of Meteorology, Long-Range Transport and Local Anthropogenic Sources. Aerosol Air Quality Research 14, 440-450.

Agarwal, A.K., Gupta, T., Dixit, N., Shukla, P.C., 2013. Assessment of toxic potential of primary and secondary particulates/aerosols from biodiesel vis-a-vis mineral diesel fuelled engine. Inhalation Toxicology 25, 325-332.

Agarwal, A.K., Gupta, T., Lukose, J., Singh, A.P., 2015. Particulate Characterization and Size Distribution in the Exhaust of a Gasoline Homogeneous Charge Compression Ignition Engine. Aerosol and Air Quality Research 15, 504-516.

Agus, E.L., Young, D.T., Lingard, J.J.N., Smalley, R.J., Tate, J.E., Goodman, P.S., Tomlin, A.S., 2007. Factors influencing particle number concentrations, size distributions and modal parameters at a roof-level and roadside site in Leicester, UK. Science of The Total Environment 386, 65-82.

Alam, A., Shi, J.P., Harrison, R.M., 2003. Observations of new particle formation in urban air. Journal of Geophysical Research 108, 4093-4107. doi:10.1029/2001JD001417

Armas, O., Gómez, A., Mata, C., Ramos, Á., 2012. Particles emitted during the stops of an urban bus fuelled with ethanol–biodiesel–diesel blends. Urban Climate 2, 43-54.

Atkinson, R.W., Fuller, G.W., Anderson, H.R., Harrison, R.M., Armstrong, B., 2010. Urban ambient particle metrics and health: a time-series analysis. Epidemiology (Cambridge, Mass.) 21, 501-511.

Bagley, S.T., Baumgard, K.J., Gratz, L.D., Johnson, J.H., Leddy, D.G., 1996. Characterization of fuel and aftertreatment device effects on diesel emissions. Research report (Health Effects Institute), 1-75; discussion 77-86.

949 Ban-Weiss, G.A., Lunden, M.M., Kirchstetter, T.W., Harley, R.A., 2010. Size-resolved particle
950 number and volume emission factors for on-road gasoline and diesel motor vehicles. Journal of
951 Aerosol Science 41, 5-12.

952 Baxla, S., Roy, A., Gupta, T., Tripathi, S., Bandyopadhyaya, R., 2009. Analysis of diurnal and
953 seasonal variation of submicron outdoor aerosol mass and size distribution in a northern Indian city
954 and its correlation to black carbon. Aerosol Air Quality Research 9, 458-469.

955 Beckerman, B., Jerrett, M., Brook, J.R., Verma, D.K., Arain, M.A., Finkelstein, M.M., 2008.
956 Correlation of nitrogen dioxide with other traffic pollutants near a major expressway. Atmospheric
957 Environment 42, 275-290.

958 Beddows, D.C., Dall'osto, M., Harrison, R.M., 2010. An enhanced procedure for the merging of
959 atmospheric particle size distribution data measured using electrical mobility and time-of-flight
960 analysers. Aerosol Science and Technology 44, 930-938.

961 Beddows, D.C.S., Dall'Osto, M., Harrison, R.M., Kulmala, M., Asmi, A., Wiedensohler, A., Laj, P.,
962 Fjaeraa, A.M., Sellegri, K., Birmili, W., Bukowiecki, N., Weingartner, E., Baltensperger, U.,
963 Zdimal, V., Zikova, N., Putaud, J.P., Marinoni, A., Tunved, P., Hansson, H.C., Fiebig, M., Kivekäs,
964 N., Swietlicki, E., Lihavainen, H., Asmi, E., Ulevicius, V., Aalto, P.P., Mihalopoulos, N., Kalivitis,
965 N., Kalapov, I., Kiss, G., de Leeuw, G., Henzing, B., O'Dowd, C., Jennings, S.G., Flentje, H.,
966 Meinhardt, F., Ries, L., Denier van der Gon, H.A.C., Visschedijk, A.J.H., 2014. Variations in
967 tropospheric submicron particle size distributions across the European continent 2008–2009.
968 Atmos. Chem. Phys. 14, 4327-4348.

969 Beddows, D.C.S., Dall'Osto, M., Harrison, R.M., 2009. Cluster Analysis of Rural, Urban, and
970 Curbside Atmospheric Particle Size Data. Environmental Science & Technology 43, 4694-4700.

971 Betha, R., Spracklen, D.V., Balasubramanian, R., 2013. Observations of new aerosol particle
972 formation in a tropical urban atmosphere. Atmospheric Environment 71, 340-351.

973 Birmili, W., Wiedensohler, A., Heintzenberg, J., Lehmann, K., 2001. Atmospheric particle number
974 size distribution in central Europe: Statistical relations to air masses and meteorology. Journal of
975 Geophysical Research: Atmospheres 106, D23, 32005-32018, doi: 10.1029/2000JD000220.

976 Biswas, S., Hu, S., Verma, V., Herner, J.D., Robertson, W.H., Ayala, A., Sioutas, C., 2008.
977 Physical properties of particulate matter (PM) from late model heavy-duty diesel vehicles operating
978 with advanced PM and NOx emission control technologies. Atmospheric Environment 42, 5622-
979 5634.

980 Brines, M., Dall'Osto, M., Beddows, D.C.S., Harrison, R.M., Querol, X., 2014. Simplifying aerosol
981 size distributions modes simultaneously detected at four monitoring sites during SAPUSS. Atmos.
982 Chem. Phys. 14, 2973-2986.

983 Brines, M., Dall'Osto, M., Beddows, D.C.S., Harrison, R.M., Gómez-Moreno, F., Núñez, L.,
984 Artíñano, B., Costabile, F., Gobbi, G.P., Salimi, F., Morawska, L., Sioutas, C., Querol, X., 2015.
985 Traffic and nucleation events as main sources of ultrafine particles in high insolation developed
986 world cities. Atmospheric Chemistry & Physics 15, 5929-5945.
987
988 Buonanno, G., Bernabei, M., Avino, P., Stabile, L., 2012. Occupational exposure to airborne
989 particles and other pollutants in an aviation base. Environmental Pollution 170, 78-87.

990 Buonanno, G., Ficco, G., Stabile, L., 2009a. Size distribution and number concentration of particles
991 at the stack of a municipal waste incinerator. Waste Management 29, 749-755.

Buonanno, G., Lall, A.A., Stabile, L., 2009b. Temporal size distribution and concentration of particles near a major highway. Atmospheric Environment 43, 1100-1105.

Buonanno, G., Morawska, L., 2015. Ultrafine particle emission of waste incinerators and comparison to the exposure of urban citizens. Waste Management 37, 75-81.

Buonanno, G., Morawska, L., Stabile, L., 2009c. Particle emission factors during cooking activities. Atmospheric Environment 43, 3235-3242.

Buonanno, G., Scungio, M., Stabile, L., Tirler, W., 2011a. Ultrafine particle emission from incinerators: The role of the fabric filter. Journal of the Air & Waste Management Association 62, 103-111.

Buonanno, G., Stabile, L., Avino, P., Belluso, E., 2011b. Chemical, dimensional and morphological ultrafine particle characterization from a waste-to-energy plant. Waste Management 31, 2253-2262.

Cadle, S., Williams, R., 1979. Gas and particle emissions from automobile tires in laboratory and field studies. Rubber Chemistry and Technology 52, 146-158.

Carbone, F., Beretta, F., D'Anna, A., 2010. Factors Influencing Ultrafine Particulate Matter (PM0. 1) Formation under Pulverized Coal Combustion and Oxyfiring Conditions. Energy & Fuels 24, 6248-6256.

Carpentieri, M., Kumar, P., 2011. Ground-fixed and on-board measurements of nanoparticles in the wake of a moving vehicle. Atmospheric Environment 45, 5837-5852.

Casati, R., Scheer, V., Vogt, R., Benter, T., 2007. Measurement of nucleation and soot mode particle emission from a diesel passenger car in real world and laboratory in situ dilution. Atmospheric Environment 41, 2125-2135.

Cernuschi, S., Giugliano, M., Ozgen, S., Consonni, S., 2012. Number concentration and chemical composition of ultrafine and nanoparticles from WTE (waste to energy) plants. Science of the Total Environment 420, 319-326.

Chakrabarty, R.K., Moosmüller, H., Garro, M.A., Arnott, W.P., Walker, J., Susott, R.A., Babbitt, R.E., Wold, C.E., Lincoln, E.N., Hao, W.M., 2006. Emissions from the laboratory combustion of wildland fuels: Particle morphology and size. Journal of Geophysical Research: Atmospheres (1984–2012) 111.

Chan, T.W., Mozurkewich, M., 2007. Application of absolute principal component analysis to size distribution data: identification of particle origins. Atmos. Chem. Phys. 7, 887-897.

Chang, M.-C.O., Chow, J.C., Watson, J.G., Hopke, P.K., Yi, S.-M., England, G.C., 2004. Measurement of ultrafine particle size distributions from coal-, oil-, and gas-fired stationary combustion sources. Journal of the Air & Waste Management Association 54, 1494-1505.

Charron, A., Birmili, W., Harrison, R.M., 2008. Fingerprinting particle origins according to their size distribution at a UK rural site. Journal of Geophysical Research: Atmospheres 113, D07202, doi:10.1029/2007JD008562.

Charron, A., Harrison, R.M., 2003. Primary particle formation from vehicle emissions during exhaust dilution in the roadside atmosphere. Atmospheric Environment 37, 4109-4119.

Cheung, H.C., Morawska, L., Ristovski, Z.D., 2011. Observation of new particle formation in subtropical urban environment. Atmospheric Chemistry & Physics 11, 3823-3833.

Costabile, F., Birmili, W., Klose, S., Tuch, T., Wehner, B., Wiedensohler, A., Franck, U., König, K., Sonntag, A., 2009. Spatio-temporal variability and principal components of the particle number size distribution in an urban atmosphere. Atmospheric Chemistry & Physics 9, 3163-3195.

Cusack, M., Pérez, N., Pey, J., Alastuey, A., Querol, X., 2013. Source apportionment of fine PM and sub-micron particle number concentrations at a regional background site in the western Mediterranean: a 2.5 year study. Atmospheric Chemistry & Physics 13, 5173-5187.

Dahl, A., Gharibi, A., Swietlicki, E., Gudmundsson, A., Bohgard, M., Ljungman, A., Blomqvist, G., Gustafsson, M., 2006. Traffic-generated emissions of ultrafine particles from pavement–tire interface. Atmospheric Environment 40, 1314-1323.

Dall'Osto, M., Thorpe, A., Beddows, D.C.S., Harrison, R.M., Barlow, J.F., Dunbar, T., Williams P.I., Coe, H., 2011a. Remarkable dynamics of nanoparticles in the urban atmosphere, Atmos. Chem. Phys. 11, 6623-6637.

Dall'Osto, M., Monahan, C., Greaney, R., Beddows, D.C.S., Harrison, R.M., Ceburnis, D., O'Dowd, C.D., 2011b. A statistical analysis of North East Atlantic (submicron) aerosol size distributions. Atmospheric Chemistry & Physics 11, 12567-12578.

Dall'Osto, M., Beddows, D.C.S., Pey, J., Rodriguez, S., Alastuey, A., Harrison, R.M., Querol, X., 2012. Urban aerosol size distributions over the Mediterranean city of Barcelona, NE Spain. Atmospheric Chemistry & Physics 12, 10693-10707.

Dall'Osto, M., Querol, X., Alastuey, A., O'Dowd, C., Harrison, R.M., Wenger, J., Gómez Moreno, F.J., 2013. On the spatial distribution and evolution of ultrafine particles in Barcelona. Atmospheric Chemistry & Physics 13, 741-759.

Dal Maso, M., Kulmala, M., Riipinen, I., Wagner, R., Hussein, T., Aalto, P.P., Lehtinen, K.E., 2005. Formation and growth of fresh atmospheric aerosols: eight years of aerosol size distribution data from SMEAR II, Hyytiala, Finland. Boreal Environment Research 10, 323-336.

Dannis, M., 1974. Rubber dust from the normal wear of tires. Rubber Chemistry and Technology 47, 1011-1037.

Dennekamp, M., Howarth, S., Dick, C., Cherrie, J., Donaldson, K., Seaton, A., 2001. Ultrafine particles and nitrogen oxides generated by gas and electric cooking. Occupational and Environmental Medicine 58, 511-516.

Dunn, M.J., Jiménez, J.-L., Baumgardner, D., Castro, T., McMurry, P.H., Smith, J.N., 2004. Measurements of Mexico City nanoparticle size distributions: Observations of new particle formation and growth. Geophysical Research Letters 31, L10102, doi: 10.1029/2004GL019483.

Dusek, U., Frank, G.P., Hildebrandt, L., Curtius, J., Schneider, J., Walter, S., Chand, D., Drewnick, F., Hings, S., Jung, D., Borrmann, S., Andreae, M.O., 2006. Size matters more than chemistry for cloud-nucleating ability of aerosol particles. Science (New York, NY) 312, 1375-1378.

Fauser, P., Tjell, J.C., Mosbaek, H., Pilegaard, K., 1999. Quantification of tire-tread particles using extractable organic zinc as tracer. Rubber Chemistry and Technology 72, 969-977.

Fitzgerald, J.W., 1991. Marine aerosols: A review. Atmospheric Environment. Part A. General Topics 25, 533-545.

Forsberg, B., Hansson, H.-C., Johansson, C., Areskoug, H., Persson, K., Järvholm, B., 2005. Comparative health impact assessment of local and regional particulate air pollutants in Scandinavia. AMBIO: Journal of the Human Environment 34, 11-19.

Friend, A., Ayoko, G., Jayaratne, E.R., Jamriska, M., Hopke, P., Morawska, L., 2012. Source apportionment of ultrafine and fine particle concentrations in Brisbane, Australia. Environmental Science Pollution Research 19, 2942-2950.

Friend, A.J., Ayoko, G.A., Jager, D., Wust, M., Jayaratne, E.R., Jamriska, M., Morawska, L., 2013. Sources of ultrafine particles and chemical species along a traffic corridor: comparison of the results from two receptor models. Environmental Chemistry 10, 54-63.

Fushimi, A., Hasegawa, S., Takahashi, K., Fujitani, Y., Tanabe, K., Kobayashi, S., 2008. Atmospheric fate of nuclei-mode particles estimated from the number concentrations and chemical composition of particles measured at roadside and background sites. Atmospheric Environment 42, 949-959.

Gao, J., Chai, F., Wang, T., Wang, S., Wang, W., 2012. Particle number size distribution and new particle formation: New characteristics during the special pollution control period in Beijing. Journal of Environmental Sciences 24, 14-21.

Gao, J., Chai, F., Wang, T., Wang, W., 2011. Particle number size distribution and new particle formation (NPF) in Lanzhou, Western China. Particuology 9, 611-618.

Garg, B.D., Cadle, S.H., Mulawa, P.A., Groblicki, P.J., Laroo, C., Parr, G.A., 2000. Brake wear particulate matter emissions. Environmental Science & Technology 34, 4463-4469.

Giechaskiel, B., Chirico, R., DeCarlo, P.F., Clairotte, M., Adam, T., Martini, G., Heringa, M.F., Richter, R., Prevot, A.S.H., Baltensperger, U., Astorga, C., 2010. Evaluation of the particle measurement programme (PMP) protocol to remove the vehicles' exhaust aerosol volatile phase. Science of the Total Environment 408, 5106-5116.

Giechaskiel, B., Ntziachristos, L., Samaras, Z., Scheer, V., Casati, R., Vogt, R., 2005. Formation potential of vehicle exhaust nucleation mode particles on-road and in the laboratory. Atmospheric Environment 39, 3191-3198.

Gogoi, M.M., Moorthy, K.K., Kompalli, S.K., Chaubey, J.P., Babu, S.S., Manoj, M., Nair, V.S., Prabhu, T.P., 2014. Physical and optical properties of aerosols in a free tropospheric environment: Results from long-term observations over western trans-Himalayas. Atmospheric Environment 84, 262-274.

Gómez-Moreno, F.J., Pujadas, M., Plaza, J., Rodríguez-Maroto, J.J., Martínez-Lozano, P., Artíñano, B., 2011. Influence of seasonal factors on the atmospheric particle number concentration and size distribution in Madrid. Atmospheric Environment 45, 3169-3180.

Gouriou, F., Morin, J.-P., Weill, M.-E., 2004. On-road measurements of particle number concentrations and size distributions in urban and tunnel environments. Atmospheric Environment 38, 2831-2840.

Gramsch, E., Gidhagen, L., Wahlin, P., Oyola, P., Moreno, F., 2009. Predominance of soot-mode ultrafine particles in Santiago de Chile: Possible sources. Atmospheric Environment 43, 2260-2267.

Gu, J., Pitz, M., Schnelle-Kreis, J., Diemer, J., Reller, A., Zimmermann, R., Soentgen, J., Stoelzel, M., Wichmann, H.E., Peters, A., Cyrys, J., 2011. Source apportionment of ambient particles:

Comparison of positive matrix factorization analysis applied to particle size distribution and chemical composition data. Atmospheric Environment 45, 1849-1857.

Gupta, T., Kothari, A., Srivastava, D.K., Agarwal, A.K., 2010. Measurement of number and size distribution of particles emitted from a mid-sized transportation multipoint port fuel injection gasoline engine. Fuel 89, 2230-2233.

Gustafsson, M., Blomqvist, G., Gudmundsson, A., Dahl, A., Swietlicki, E., Bohgard, M., Lindbom, J., Ljungman, A., 2008. Properties and toxicological effects of particles from the interaction between tyres, road pavement and winter traction material. Science of the Total Environment 393, 226-240.

Guyon, P., Frank, G., Welling, M., Chand, D., Artaxo, P., Rizzo, L., Nishioka, G., Kolle, O., Fritsch, H., Dias, S., 2005. Airborne measurements of trace gas and aerosol particle emissions from biomass burning in Amazonia. Atmospheric Chemistry & Physics 5, 2989-3002.

Hagler, G.S.W., Baldauf, R.W., Thoma, E.D., Long, T.R., Snow, R.F., Kinsey, J.S., Oudejans, L., Gullett, B.K., 2009. Ultrafine particles near a major roadway in Raleigh, North Carolina: Downwind attenuation and correlation with traffic-related pollutants. Atmospheric Environment 43, 1229-1234.

Hallquist, Å.M., Fridell, E., Westerlund, J., Hallquist, M., 2012. Onboard Measurements of Nanoparticles from a SCR-Equipped Marine Diesel Engine. Environmental science & Technology 47, 773-780.

Harris, S.J., Maricq, M.M., 2001. Signature size distributions for diesel and gasoline engine exhaust particulate matter. Journal of Aerosol Science 32, 749-764.

Harrison, R.M., Beddows, D.C.S., Dall'Osto, M., 2011. PMF Analysis of Wide-Range Particle Size Spectra Collected on a Major Highway. Environmental Science & Technology 45, 5522-5528.

Harrison, R.M., Jones, M., Collins, G., 1999. Measurements of the physical properties of particles in the urban atmosphere. Atmospheric Environment 33, 309-321.

Harrison, R.M., Shi, J.P., Xi, S., Khan, A., Mark, D., Kinnersley, R., Yin, J., 2000. Measurement of Number, Mass and Size Distribution of Particles in the Atmosphere. Philosophical Transactions: Mathematical, Physical and Engineering Sciences 358, 2567-2580.

Harrison, R.M., Yin, J., Mark, D., Stedman, J., Appleby, R.S., Booker, J., Moorcroft, S., 2001. Studies of the coarse particle (2.5–10μm) component in UK urban atmospheres. Atmospheric Environment 35, 3667-3679.

He, C., Morawska, L., Hitchins, J., Gilbert, D., 2004. Contribution from indoor sources to particle number and mass concentrations in residential houses. Atmospheric Environment 38, 3405-3415.

HEI_Review_Panel, 2013. Understanding the Health Effects of Ambient Ultrafine Particles, HEI Perspectives 3. Health Effects Institute, Boston, MA.

Heintzenberg, J., Covert, D., Van Dingenen, R., 2000. Size distribution and chemical composition of marine aerosols: a compilation and review. Tellus B 52, 1104-1122.

Herndon, S.C., Jayne, J.T., Lobo, P., Onasch, T.B., Fleming, G., Hagen, D.E., Whitefield, P.D., Miake-Lye, R.C., 2008. Commercial aircraft engine emissions characterization of in-use aircraft at Hartsfield-Jackson Atlanta International Airport. Environmental Science & Technology 42, 1877-1883.

1154 Hinds, W.C., 1999. Aerosol Technology: Properties. Behavior, and Measurement of airborne
1155 Particles (2nd edition).

1156 Hitchins, J., Morawska, L., Wolff, R., Gilbert, D., 2000. Concentrations of submicrometre particles
1157 from vehicle emissions near a major road. Atmospheric Environment 34, 51-59.

1158 Holmes, N.S., 2007. A review of particle formation events and growth in the atmosphere in the
1159 various environments and discussion of mechanistic implications. Atmospheric Environment 41,
1160 2183-2201.

1161 Hopke, P.K., 2003. Recent developments in receptor modeling. Journal of Chemometrics 17, 255-
1162 265.

1163 Hoppel, W., Frick, G., Fitzgerald, J., Larson, R., 1994a. Marine boundary layer measurements of
1164 new particle formation and the effects nonprecipitating clouds have on aerosol size distribution.
1165 Journal of Geophysical Research: Atmospheres 99, D7 14443-14459, doi: 10.1029/94JD00797.

1166 Hoppel, W., Frick, G., Fitzgerald, J., Wattle, B., 1994b. A cloud chamber study of the effect that
1167 nonprecipitating water clouds have on the aerosol size distribution. Aerosol Science & Technology
1168 20, 1-30.

1169 Hosseini, S., Li, Q., Cocker, D., Weise, D., Miller, A., Shrivastava, M., Miller, J., Mahalingam, S.,
1170 Princevac, M., Jung, H., 2010. Particle size distributions from laboratory-scale biomass fires using
1171 fast response instruments. Atmospheric Chemistry & Physics 10, 8065-8076.

1172 Huang, C., Lou, D., Hu, Z., Feng, Q., Chen, Y., Chen, C., Tan, P., Yao, D., 2013. A PEMS study of
1173 the emissions of gaseous pollutants and ultrafine particles from gasoline- and diesel-fueled vehicles.
1174 Atmospheric Environment 77, 703-710.

1175 Hussein, T., Glytsos, T., Ondráček, J., Dohányosová, P., Ždímal, V., Hämeri, K., Lazaridis, M.,
1176 Smolík, J., Kulmala, M., 2006a. Particle size characterization and emission rates during indoor
1177 activities in a house. Atmospheric Environment 40, 4285-4307.

1178 Hussein, T., Hämeri, K., Aalto, P.P., Paatero, P., Kulmala, M., 2005. Modal structure and spatial–
1179 temporal variations of urban and suburban aerosols in Helsinki—Finland. Atmospheric
1180 Environment 39, 1655-1668.

1181 Hussein, T., Karppinen, A., Kukkonen, J., Härkönen, J., Aalto, P.P., Hämeri, K., Kerminen, V.-M.,
1182 Kulmala, M., 2006b. Meteorological dependence of size-fractionated number concentrations of
1183 urban aerosol particles. Atmospheric Environment 40, 1427-1440.

1184 ICRP, 1994. ICRP Publication 66: Human Respiratory Tract Model for Radiological Protection.
1185 Elsevier Health Sciences.

1186 Iijima, A., Sato, K., Yano, K., Kato, M., Kozawa, K., Furuta, N., 2008. Emission factor for
1187 antimony in brake abrasion dusts as one of the major atmospheric antimony sources. Environmental
1188 Science & Technology 42, 2937-2942.

1189 Iijima, A., Sato, K., Yano, K., Tago, H., Kato, M., Kimura, H., Furuta, N., 2007. Particle size and
1190 composition distribution analysis of automotive brake abrasion dusts for the evaluation of antimony
1191 sources of airborne particulate matter. Atmospheric Environment 41, 4908-4919.

1192 Jacobson, M.Z., Seinfeld, J.H., 2004. Evolution of nanoparticle size and mixing state near the point
1193 of emission. Atmospheric Environment 38, 1839-1850.

1194 Janhäll, S., Andreae, M.O., Pöschl, U., 2010. Biomass burning aerosol emissions from vegetation
1195 fires: particle number and mass emission factors and size distributions. Atmospheric Chemistry &
1196 Physics 10, 1427-1439.

1197 Jeong, C.-H., Hopke, P.K., Chalupa, D., Utell, M., 2004. Characteristics of Nucleation and Growth
1198 Events of Ultrafine Particles Measured in Rochester, NY. Environmental Science & Technology 38,
1199 1933-1940.

1200 Jeong, C.-H., Evans, G.J., 2009. Inter-comparison of a fast mobility particle sizer and a scanning
1201 mobility particle sizer incorporating an ultrafine water-based condensation particle counter. Aerosol
1202 Science & Technology 43, 364-373.

1203 Jeong, C.-H., Evans, G.J., Hopke, P.K., Chalupa, D.J., Utell, M., 2006. Influence of atmospheric
1204 dispersion and new particle formation events on ambient particle number concentration in
1205 Rochester, United States, and Toronto, Canada. Journal of the Air & Waste Management
1206 Association 56, 431-443.

1207 Jones, A.M., Harrison, R.M., Barratt, B., Fuller, G., 2012. A large reduction in airborne particle
1208 number concentrations at the time of the introduction of “sulphur free” diesel and the London Low
1209 Emission Zone. Atmospheric Environment 50, 129-138.

1210 Jonsson, Å.M., Westerlund, J., Hallquist, M., 2011. Size-resolved particle emission factors for
1211 individual ships. Geophysical Research Letters 38, doi: 10.1029/2011GL047672.

1212 Joshi, M., Sapra, B.K., Khan, A., Tripathi, S.N., Shamjad, P.M., Gupta, T., Mayya, Y.S., 2012.
1213 Harmonisation of nanoparticle concentration measurements using GRIMM and TSI scanning
1214 mobility particle sizers. Journal of Nanoparticle Research 14, 1-14.

1215 Joutsensaari, J., Kauppinen, E.I., Ahonen, P., Lind, T.M., Ylätalo, S.I., Jokiniemi, J.K., Hautanen,
1216 J., Kilpeläinen, M., 1992. Aerosol formation in real scale pulverized coal combustion. Journal of
1217 Aerosol Science 23, 241-244.

1218 Kaminski, H., Kuhlbusch, T.A., Rath, S., Götz, U., Sprenger, M., Wels, D., Polloczek, J.,
1219 Bachmann, V., Dziurowitz, N., Kiesling, H.-J., 2013. Comparability of mobility particle sizers and
1220 diffusion chargers. Journal of Aerosol Science 57, 156-178.

1221 Kasper, A., Aufdenblatten, S., Forss, A., Mohr, M., Burtscher, H., 2007. Particulate emissions from
1222 a low-speed marine diesel engine. Aerosol Science and Technology 41, 24-32.

1223 Kasumba, J., Hopke, P.K., Chalupa, D.C., Utell, M.J., 2009. Comparison of sources of submicron
1224 particle number concentrations measured at two sites in Rochester, NY. Science of The Total
1225 Environment 407, 5071-5084.

1226 Kaul, D., Gupta, T., Tripathi, S., Tare, V., Collett Jr, J., 2011. Secondary organic aerosol: a
1227 comparison between foggy and nonfoggy days. Environmental Science & Technology 45, 7307-
1228 7313.

1229 Ketzel, M., Wåhlin, P., Berkowicz, R., Palmgren, F., 2003. Particle and trace gas emission factors
1230 under urban driving conditions in Copenhagen based on street and roof-level observations.
1231 Atmospheric Environment 37, 2735-2749.

1232 Kim, E., Hopke, P.K., Larson, T.V., Covert, D.S., 2003. Analysis of Ambient Particle Size
1233 Distributions Using Unmix and Positive Matrix Factorization. Environmental Science &
1234 Technology 38, 202-209.

1235 Kinsey, J.S., Dong, Y., Williams, D.C., Logan, R., 2010. Physical characterization of the fine
1236 particle emissions from commercial aircraft engines during the Aircraft Particle Emissions
1237 eXperiment (APEX) 1–3. Atmospheric Environment 44, 2147-2156.

1238 Kirchstetter, T., Harley, R.A., Kreisberg, N.M., Stolzenburg, M.R., Hering, S.V., 1999. On-road
1239 measurement of fine particle and nitrogen oxide emissions from light-and heavy-duty motor
1240 vehicles. Atmospheric Environment 33, 2955-2968.

1241 Kittelson, D., Watts, W., Johnson, J., 2002. Diesel Aerosol Sampling Methodology–CRC E-43.
1242 Final report, Coordinating Research Council.

1243 Kittelson, D.B., Watts, W.F., Johnson, J.P., 2004. Nanoparticle emissions on Minnesota highways.
1244 Atmospheric Environment 38, 9-19.

1245 Knibbs, L.D., de Dear, R.J., Morawska, L., Mengersen, K.L., 2009. On-road ultrafine particle
1246 concentration in the M5 East road tunnel, Sydney, Australia. Atmospheric Environment 43, 3510-
1247 3519.

1248 Koponen, I.K., Virkkula, A., Hillamo, R., Kerminen, V.M., Kulmala, M., 2002. Number size
1249 distributions and concentrations of marine aerosols: Observations during a cruise between the
1250 English Channel and the coast of Antarctica. Journal of Geophysical Research: Atmospheres
1251 (1984–2012) 107, AAC 6-1-AAC 6-8, doi/10.1029/2002JD002533.

1252 Kukutschová, J., Moravec, P., Tomášek, V., Matějka, V., Smolík, J., Schwarz, J., Seidlerová, J.,
1253 Šafářová, K., Filip, P., 2011. On airborne nano/micro-sized wear particles released from low-
1254 metallic automotive brakes. Environmental Pollution 159, 998-1006.

1255 Kulmala, M., Vehkamäki, H., Petäjä, T., Dal Maso, M., Lauri, A., Kerminen, V.-M., Birmili, W.,
1256 McMurry, P.H., 2004. Formation and growth rates of ultrafine atmospheric particles: a review of
1257 observations. Journal of Aerosol Science 35, 143-176.

1258 Kulmala, M., Petäjä, T., Nieminen, T., Sipilä, M., Manninen, H.E., Lehtipalo, K., Dal Maso, M.,
1259 Aalto, P.P., H. Junninen, Paasonen, P., Riipinen, I., Lehtinen, K.E.J., Laaksonen, A., Kerminen, V.-
1260 M., 2012. Measurement of the nucleation of atmospheric aerosol particles. Nature Protocol 7,
1261 1651-1667, doi:10.1038/nprot.2012.091.
1262
1263 Kumar, P., Pirjola, L., Ketzel, M., Harrison, R.M., 2013. Nanoparticle emissions from 11 non-
1264 vehicle exhaust sources–A review. Atmospheric Environment 67, 252-277.

1265 Kumar, P., Ketzel, M., Vardoulakis, S., Pirjola, L., Britter, R., 2011. Dynamics and dispersion
1266 modelling of nanoparticles from road traffic in the urban atmospheric environment—a review.
1267 Journal of Aerosol Science 42, 580-603.

1268 Kwak, J., Lee, S., Lee, S., 2014. On-road and laboratory investigations on non-exhaust ultrafine
1269 particles from the interaction between the tire and road pavement under braking conditions.
1270 Atmospheric Environment 97, 195-205.

1271 Lenschow, P., Abraham, H.J., Kutzner, K., Lutz, M., Preuß, J.D., Reichenbächer, W., 2001. Some
1272 ideas about the sources of PM10. Atmospheric Environment 35, Supplement 1, S23-S33.

1273 Li, C.-S., Lin, W.-H., Jenq, F.-T., 1993. Size distributions of submicrometer aerosols from cooking.
1274 Environment International 19, 147-154.

Li, T., Chen, X., Yan, Z., 2013. Comparison of fine particles emissions of light-duty gasoline vehicles from chassis dynamometer tests and on-road measurements. Atmospheric Environment 68, 82-91.

Li, X., Wang, J., Tu, X., Liu, W., Huang, Z., 2007. Vertical variations of particle number concentration and size distribution in a street canyon in Shanghai, China. Science of the Total Environment 378, 306-316.

Li, Y., Suriyawong, A., Daukoru, M., Zhuang, Y., Biswas, P., 2009. Measurement and capture of fine and ultrafine particles from a pilot-scale pulverized coal combustor with an electrostatic precipitator. Journal of the Air & Waste Management Association 59, 553.

Liang, B., Ge, Y., Tan, J., Han, X., Gao, L., Hao, L., Ye, W., Dai, P., 2013. Comparison of PM emissions from a gasoline direct injected (GDI) vehicle and a port fuel injected (PFI) vehicle measured by electrical low pressure impactor (ELPI) with two fuels: Gasoline and M15 methanol gasoline. Journal of Aerosol Science 57, 22-31.

Lighty, J.S., Veranth, J.M., Sarofim, A.F., 2000. Combustion aerosols: factors governing their size and composition and implications to human health. Journal of the Air & Waste Management Association 50, 1565-1618.

Linak, W.P., Peterson, T.W., 1984. Effect of coal type and residence time on the submicron aerosol distribution from pulverized coal combustion. Aerosol Science and Technology 3, 77-96.

Lingard, J.J., Agus, E.L., Young, D.T., Andrews, G.E., Tomlin, A.S., 2006. Observations of urban airborne particle number concentrations during rush-hour conditions: analysis of the number based size distributions and modal parameters. Journal of Environmental Monitoring 8, 1203-1218.

Lipsky, E., Stanier, C.O., Pandis, S.N., Robinson, A.L., 2002. Effects of sampling conditions on the size distribution of fine particulate matter emitted from a pilot-scale pulverized-coal combustor. Energy & Fuels 16, 302-310.

Lipsky, E.M., Pekney, N.J., Walbert, G.F., O'Dowd, W.J., Freeman, M.C., Robinson, A., 2004. Effects of dilution sampling on fine particle emissions from pulverized coal combustion. Aerosol Science and Technology 38, 574-587.

Longley, I., Gallagher, M., Dorsey, J., Flynn, M., Allan, J., Alfarra, M., Inglis, D., 2003. A case study of aerosol (4.6 nm<Dp< 10μm) number and mass size distribution measurements in a busy street canyon in Manchester, UK. Atmospheric Environment 37, 1563-1571.

Manninen, H., Nieminen, T., Asmi, E., Gagné, S., Häkkinen, S., Lehtipalo, K., Aalto, P., Vana, M., Mirme, A., Mirme, S., 2010. EUCAARI ion spectrometer measurements at 12 European sites–analysis of new particle formation events. Atmospheric Chemistry & Physics 10, 7907-7927.

Maguhn, J., Karg, E., Kettrup, A., Zimmermann, R., 2003. On-line analysis of the size distribution of fine and ultrafine aerosol particles in flue and stack gas of a municipal waste incineration plant: effects of dynamic process control measures and emission reduction devices. Environmental Science & Technology 37, 4761-4770.

Mäkelä, J.M., Koponen, I.K., Aalto, P., Kulmala, M., 2000. One year data of submicron size modes of tropopheric background aerosol in southern Finland. Journal of Aerosol Science 31, 595-611.

Maricq, M.M., Chase, R.E., Xu, N., 2001. A comparison of tailpipe, dilution tunnel, and wind tunnel data in measuring motor vehicle PM. Journal of the Air & Waste Management Association 51, 1529-1537.

1317 Mathissen, M., Scheer, V., Vogt, R., Benter, T., 2011. Investigation on the potential generation of
1318 ultrafine particles from the tire–road interface. Atmospheric Environment 45, 6172-6179.

1319 Mayer, A., Czerwinski, J., Legerer, F., Wyser, M., 2002. VERT particulate trap verification. SAE
1320 Technical Paper.

1321 Mazaheri, M., Johnson, G.R., Morawska, L., 2008. Particle and gaseous emissions from
1322 commercial aircraft at each stage of the landing and takeoff cycle. Environmental Science &
1323 Technology 43, 441-446.

1324 Meyer, N.K., Ristovski, Z., 2007. Ternary nucleation as a mechanism for the production of diesel
1325 nanoparticles: Experimental analysis of the volatile and hygroscopic properties of diesel exhaust
1326 using the volatilization and humidification tandem differential mobility analyzer. Environmental
1327 Science & Technology 41, 7309-7314.

1328 Mohr, M., Ylätalo, S., Klippel, N., Kauppinen, E., Riccius, O., Burtscher, H., 1996. Submicron fly
1329 ash penetration through electrostatic precipitators at two coal power plants. Aerosol Science and
1330 Technology 24, 191-204.

1331 Mönkkönen, P., Uma, R., Srinivasan, D., Koponen, I., Lehtinen, K., Hämeri, K., Suresh, R.,
1332 Sharma, V., Kulmala, M., 2004. Relationship and variations of aerosol number and PM< sub>
1333 10</sub> mass concentrations in a highly polluted urban environment—New Delhi, India.
1334 Atmospheric Environment 38, 425-433.

1335 Morawska, L., Jayaratne, E., Mengersen, K., Jamriska, M., Thomas, S., 2002. Differences in
1336 airborne particle and gaseous concentrations in urban air between weekdays and weekends.
1337 Atmospheric Environment 36, 4375-4383.

1338 Morawska, L., Johnson, G.R., He, C., Ayoko, G.A., Lim, M., Swanson, C., Ristovski, Z., Moore,
1339 M., 2006. Particle number emissions and source signatures of an industrial facility. Environmental
1340 Science & Technology 40, 803-814.

1341 Morawska, L., Ristovski, Z., Jayaratne, E.R., Keogh, D.U., Ling, X., 2008. Ambient nano and
1342 ultrafine particles from motor vehicle emissions: Characteristics, ambient processing and
1343 implications on human exposure. Atmospheric Environment 42, 8113-8138.

1344 Morawska, L., Thomas, S., Jamriska, M., Johnson, G., 1999. The modality of particle size
1345 distributions of environmental aerosols. Atmospheric Environment 33, 4401-4411.

1346 Mosleh, M., Blau, P.J., Dumitrescu, D., 2004. Characteristics and morphology of wear particles
1347 from laboratory testing of disk brake materials. Wear 256, 1128-1134.

1348 Myung, C.L., Park, S., 2012. Exhaust nanoparticle emissions from internal combustion engines: A
1349 review. International Journal of Automotive Technology 13, 9-22.

1350 Nieto, P.G., García, B.A., Diaz, J.F., Brana, M.R., 1994. Parametric study of selective removal of
1351 atmospheric aerosol by below-cloud scavenging. Atmospheric Environment 28, 2335-2342.

1352 Ning, Z., Hudda, N., Daher, N., Kam, W., Herner, J., Kozawa, K., Mara, S., Sioutas, C., 2010.
1353 Impact of roadside noise barriers on particle size distributions and pollutants concentrations near
1354 freeways. Atmospheric Environment 44, 3118-3127.

1355 Noble, C.A., Mukerjee, S., Gonzales, M., Rodes, C.E., Lawless, P.A., Natarajan, S., Myers, E.A.,
1356 Norris, G.A., Smith, L., Özkaynak, H., 2003. Continuous measurement of fine and ultrafine
1357 particulate matter, criteria pollutants and meteorological conditions in urban El Paso, Texas.
1358 Atmospheric Environment 37, 827-840.

O'Dowd, C.D., Smith, M.H., Consterdine, I.E., Lowe, J.A., 1997. Marine aerosol, sea-salt, and the marine sulphur cycle: A short review. Atmospheric Environment 31, 73-80.

Oberdörster, G., Elder, A., Finkelstein, J., Frampton, M., Hopke, P.K., Peters, A., Prather, K., Wichmann, E., Utell, M., 2010. Assessment of Ambient UFP Health Effects: Linking Sources to Exposure and Responses in Extrapulmonary Organs. Rochester PM Center Report. Grant EPA R827354. Ultrafine particles: Characterization, Health Effects and Pathophysiological Mechanisms. 1999 - 2005

Ogulei, D., Hopke, P., Wallace, L., 2006a. Analysis of indoor particle size distributions in an occupied townhouse using positive matrix factorization. Indoor Air 16, 204-215.

Ogulei, D., Hopke, P.K., Chalupa, D.C., Utell, M.J., 2007. Modeling source contributions to submicron particle number concentrations measured in Rochester, New York. Aerosol Science and Technology 41, 179-201.

Ogulei, D., Hopke, P.K., Zhou, L., Patrick Pancras, J., Nair, N., Ondov, J.M., 2006b. Source apportionment of Baltimore aerosol from combined size distribution and chemical composition data. Atmospheric Environment 40, 396-410.

Ohlström, M.O., Lehtinen, K.E., Moisio, M., Jokiniemi, J.K., 2000. Fine-particle emissions of energy production in Finland. Atmospheric Environment 34, 3701-3711.

Olofsson, U., 2011. A study of airborne wear particles generated from the train traffic—Block braking simulation in a pin-on-disc machine. Wear 271, 86-91.

Ozgen, S., Ripamonti, G., Cernuschi, S., Giugliano, M., 2012. Ultrafine particle emissions for municipal waste-to-energy plants and residential heating boilers. Reviews in Environmental Science and Bio/Technology 11, 407-415.

Paatero, P., Tapper, U., 1994. Positive matrix factorization: A non-negative factor model with optimal utilization of error estimates of data values. Environmetrics 5, 111-126.

Peters, A., Wichmann, H.E., Tuch, T., Heinrich, J., Heyder, J., 1997. Respiratory effects are associated with the number of ultrafine particles. American Journal of Respiratory and Critical Care Medicine 155, 1376-1383.

Petzold, A., Hasselbach, J., Lauer, P., Baumann, R., Franke, K., Gurk, C., Schlager, H., Weingartner, E., 2008. Experimental studies on particle emissions from cruising ship, their characteristic properties, transformation and atmospheric lifetime in the marine boundary layer. Atmospheric Chemistry & Physics 8, 2387-2403.

Pey, J., Querol, X., Alastuey, A., Rodríguez, S., Putaud, J.P., Van Dingenen, R., 2009. Source apportionment of urban fine and ultra-fine particle number concentration in a Western Mediterranean city. Atmospheric Environment 43, 4407-4415.

Pitts, B.F., Pitts, J., 2000. Chemistry of the upper and lower atmosphere: Theory, Experiments, and Applications. Academic Press New York, NY,, USA.

Raes, F., Van Dingenen, R., Cuevas, E., Van Velthoven, P.F., Prospero, J.M., 1997. Observations of aerosols in the free troposphere and marine boundary layer of the subtropical Northeast Atlantic: Discussion of processes determining their size distribution. Journal of Geophysical Research: Atmospheres (1984–2012) 102, 21315-21328, doi: 10.1029/97JD01122.

Reche, C., Querol, X., Alastuey, A., Viana, M., Pey, J., Moreno, T., Rodríguez, S., González, Y., Fernández-Camacho, R., de la Rosa, J., Dall'Osto, M., Prévôt, A.S.H., Hueglin, C., Harrison, R.M.,

1401 Quincey, P., 2011. New considerations for PM, Black Carbon and particle number concentration for
1402 air quality monitoring across different European cities. Atmospheric Chemistry & Phyics 11, 6207-
1403 6227.

1404 Reid, J., Koppmann, R., Eck, T., Eleuterio, D., 2005. A review of biomass burning emissions part
1405 II: intensive physical properties of biomass burning particles. Atmospheric Chemistry and Physics
1406 5, 799-825.

1407 Reid, J.S., Hobbs, P.V., 1998. Physical and optical properties of young smoke from individual
1408 biomass fires in Brazil. Journal of Geophysical Research: Atmospheres (1984–2012) 103, 32013-
1409 32030.

1410 Reid, J.S., Hobbs, P.V., Ferek, R.J., Blake, D.R., Martins, J.V., Dunlap, M.R., Liousse, C., 1998.
1411 Physical, chemical, and optical properties of regional hazes dominated by smoke in Brazil. Journal
1412 of Geophysical Research: Atmospheres 103, D24, 32059-32080, doi: 10.1029/98JD00458.

1413 Ristovski, Z., Jayaratne, E., Lim, M., Ayoko, G.A., Morawska, L., 2006. Influence of diesel fuel
1414 sulfur on nanoparticle emissions from city buses. Environmental Science & Technology 40, 1314-
1415 1320.

1416 Rogers, F., Arnott, P., Zielinska, B., Sagebiel, J., Kelly, K.E., Wagner, D., Lighty, J.S., Sarofim,
1417 A.F., 2005. Real-time measurements of jet aircraft engine exhaust. Journal of the Air & Waste
1418 Management Association 55, 583-593.

1419 Rose, D., Nowak, A., Achtert, P., Wiedensohler, A., Hu, M., Shao, M., Zhang, Y., Andreae, M.,
1420 Poschl, U., 2010. Cloud condensation nuclei in polluted air and biomass burning smoke near the
1421 mega-city Guangzhou, China-Part 1: size resolved measurements and implications for the
1422 modelling of aerosol particle hygroscopicity and CCN activity. Atmospheric Chemistry & Physics
1423 10, 3365-3383.

1424 Sanders, P.G., Xu, N., Dalka, T.M., Maricq, M.M., 2003. Airborne brake wear debris: size
1425 distributions, composition, and a comparison of dynamometer and vehicle tests. Environmental
1426 Science & Technology 37, 4060-4069.

1427 See, S.W., Balasubramanian, R., 2006. Physical characteristics of ultrafine particles emitted from
1428 different gas cooking methods. Aerosol and Air Quality Research 6, 82-92.

1429 Seinfeld, J., Pandis, S., 1998. Atmospheric Chemistry and Physics, 1326 pp. John Wiley, Hoboken,
1430 NJ.

1431 Sellegri, K., Laj, P., Venzac, H., Boulon, J., Picard, D., Villani, P., Bonasoni, P., Marinoni, A.,
1432 Cristofanelli, P., Vuillermoz, E., 2010. Seasonal variations of aerosol size distributions based on
1433 long-term measurements at the high altitude Himalayan site of Nepal Climate Observatory-Pyramid
1434 (5079 m), Nepal. Atmospheric Chemistry & Physics Discussions 10, 6537-6566.

1435 Shi, J.P., Harrison, R.M., 1999. Investigation of Ultrafine Particle Formation during Diesel Exhaust
1436 Dilution. Environmental Science & Technology 33, 3730-3736.

1437 Shi, J.P., Khan, A., Harrison, R.M., 1999. Measurements of ultrafine particle concentration and size
1438 distribution in the urban atmosphere. Science of the Total Environment 235, 51-64.

1439 Shi, J.P., Mark, D., Harrison, R.M., 2000. Characterization of particles from a current technology
1440 heavy-duty diesel engine. Environmental Science & Technology 34, 748-755.

1441 Stanier, C.O., Khlystov, A.Y., Pandis, S.N., 2004a. Ambient aerosol size distributions and number
1442 concentrations measured during the Pittsburgh Air Quality Study (PAQS). Atmospheric
1443 Environment 38, 3275-3284.

1444 Stanier, C.O., Khlystov, A.Y., Pandis, S.N., 2004b. Nucleation events during the Pittsburgh Air
1445 Quality Study: description and relation to key meteorological, gas phase, and aerosol parameters
1446 special issue of aerosol science and technology on findings from the fine particulate matter
1447 supersites program. Aerosol Science & Technology 38, 253-264.

1448 Suriyawong, A., Gamble, M., Lee, M.-H., Axelbaum, R., Biswas, P., 2006. Submicrometer particle
1449 formation and mercury speciation under O2-CO2 coal combustion. Energy & Fuels 20, 2357-2363.

1450 Swietlicki, E., Hansson, H.C., Hämeri, K., Svenningsson, B., Massling, A., McFiggans, G.,
1451 McMurry, P., Petäjä, T., Tunved, P., Gysel, M., 2008. Hygroscopic properties of submicrometer
1452 atmospheric aerosol particles measured with H-TDMA instruments in various environments—A
1453 review. Tellus B 60, 432-469.

1454 Thimmaiah, D., Hovorka, J., Hopke, P.K., 2009. Source apportionment of winter submicron Prague
1455 aerosols from combined particle number size distribution and gaseous composition data. Aerosol
1456 and Air Quality Research 9, 209-236.

1457 Thorpe, A., Harrison, R.M., 2008. Sources and properties of non-exhaust particulate matter from
1458 road traffic: a review. Science of the Total Environment 400, 270-282.

1459 Thorpe, A.J., Harrison, R.M., Boulter, P.G., McCrae, I.S., 2007. Estimation of particle resuspension
1460 source strength on a major London Road. Atmospheric Environment 41, 8007-8020.

1461 Tobias, H.J., Beving, D.E., Ziemann, P.J., Sakurai, H., Zuk, M., McMurry, P.H., Zarling, D.,
1462 Waytulonis, R., Kittelson, D.B., 2001. Chemical Analysis of Diesel Engine Nanoparticles Using a
1463 Nano-DMA/Thermal Desorption Particle Beam Mass Spectrometer. Environmental Science &
1464 Technology 35, 2233-2243.

1465 Tunved, P., Ström, J., Hansson, H.C., 2004. An investigation of processes controlling the evolution
1466 of the boundary layer aerosol size distribution properties at the Swedish background station
1467 Aspvreten. Atmospheric Chemistry & Physics 4, 2581-2592.

1468 Väkevä, M., Hämeri, K., Puhakka, T., Nilsson, E.D., Hohti, H., Mäkelä, J.M., 2000. Effects of
1469 meteorological processes on aerosol particle size distribution in an urban background area. Journal
1470 of Geophysical Research: Atmospheres 105, D8, 9807-9821, doi: 10.1029/1999JD901143.

1471 Viana, M., Kuhlbusch, T.A.J., Querol, X., Alastuey, A., Harrison, R.M., Hopke, P.K., Winiwarter,
1472 W., Vallius, M., Szidat, S., Prévôt, A.S.H., Hueglin, C., Bloemen, H., Wåhlin, P., Vecchi, R.,
1473 Miranda, A.I., Kasper-Giebl, A., Maenhaut, W., Hitzenberger, R., 2008. Source apportionment of
1474 particulate matter in Europe: A review of methods and results. Journal of Aerosol Science 39, 827-
1475 849.

1476 Vogt, R., Scheer, V., Casati, R., Benter, T., 2003. On-road measurement of particle emission in the
1477 exhaust plume of a diesel passenger car. Environmental Science & Technology 37, 4070-4076.

1478 Von Bismarck-Osten, C., Birmili, W., Ketzel, M., Massling, A., Petäjä, T., Weber, S., 2013.
1479 Characterization of parameters influencing the spatio-temporal variability of urban particle number
1480 size distributions in four European cities. Atmospheric Environment 77, 415-429.

1481 von Klot, S., Peters, A., Aalto, P., Bellander, T., Berglind, N., D'Ippoliti, D., Elosua, R., Hörmann,
1482 A., Kulmala, M., Lanki, T., 2005. Ambient air pollution is associated with increased risk of hospital

cardiac readmissions of myocardial infarction survivors in five European cities. Circulation 112, 3073-3079.

Wåhlin, P., Berkowicz, R., Palmgren, F., 2006. Characterisation of traffic-generated particulate matter in Copenhagen. Atmospheric Environment 40, 2151-2159.

Wahlström, J., Olander, L., Olofsson, U., 2010a. Size, shape, and elemental composition of airborne wear particles from disc brake materials. Tribology Letters 38, 15-24.

Wahlström, J., Söderberg, A., Olander, L., Jansson, A., Olofsson, U., 2010b. A pin-on-disc simulation of airborne wear particles from disc brakes. Wear 268, 763-769.

Wahlström, J., Olofsson, U., 2015. A field study of airborne particle emissions from automotive disc brakes. Proceedings of the Institution of Mechanical Engineers, Part D: Journal of Automobile Engineering, 229, 747-757.

Wahlström, J., Söderberg, A., Olander, L., Olofsson, U., 2009. A disc brake test stand for measurement of airborne wear particles. Lubrication Science 21, 241-252.

Wallace, L., 2006. Indoor Sources of Ultrafine and Accumulation Mode Particles: Size Distributions, Size-Resolved Concentrations, and Source Strengths. Aerosol Science & Technology 40, 348-360.

Wang, H.L., Hao, Z.P., Zhuang, Y.H., Wang, W., Liu, X.Y., 2008. Characterization of inorganic components of size-segregated particles in the flue gas of a coal-fired power plant. Energy & Fuels 22, 1636-1640.

Wang, Y., Hopke, P.K., Chalupa, D.C., Utell, M.J., 2011a. Effect of the shutdown of a coal-fired power plant on urban ultrafine particles and other pollutants. Aerosol Science & Technology 45, 1245-1249.

Wang, Y., Hopke, P.K., Chalupa, D.C., Utell, M.J., 2011b. Long-term study of urban ultrafine particles and other pollutants. Atmospheric Environment 45, 7672-7680.

Wang, Z.B., Hu, M., Wu, Z.J., Yue, D.L., He, L.Y., Huang, X.F., Liu, X.G., Wiedensohler, A., 2013. Long-term measurements of particle number size distributions and the relationships with air mass history and source apportionment in the summer of Beijing. Atmospheric Chemistry & Physics Discussion 13, 5165-5197.

Wardoyo, A.Y., Morawska, L., Ristovski, Z.D., Marsh, J., 2006. Quantification of particle number and mass emission factors from combustion of Queensland trees. Environmental Science & Technology 40, 5696-5703.

Wegner, T., Hussein, T., Hämeri, K., Vesala, T., Kulmala, M., Weber, S., 2012. Properties of aerosol signature size distributions in the urban environment as derived by cluster analysis. Atmospheric Environment 61, 350-360.

Wehner, B., Birmili, W., Gnauk, T., Wiedensohler, A., 2002. Particle number size distributions in a street canyon and their transformation into the urban-air background: measurements and a simple model study. Atmospheric Environment 36, 2215-2223.

Wehner, B., Uhrner, U., Von Löwis, S., Zallinger, M., Wiedensohler, A., 2009. Aerosol number size distributions within the exhaust plume of a diesel and a gasoline passenger car under on-road conditions and determination of emission factors. Atmospheric Environment 43, 1235-1245.

Wehner, B., Wiedensohler, A., Tuch, T., Wu, Z., Hu, M., Slanina, J., Kiang, C., 2004. Variability of the aerosol number size distribution in Beijing, China: New particle formation, dust storms, and high continental background. Geophysical Research Letters 31, L22108, doi:10.1029/2004GL021596.

Weingartner, E., Burtscher, H., Baltensperger, U., 1997. Hygroscopic properties of carbon and diesel soot particles. Atmospheric Environment 31, 2311-2327.

Westerdahl, D., Wang, X., Pan, X., Zhang, K.M., 2009. Characterization of on-road vehicle emission factors and microenvironmental air quality in Beijing, China. Atmospheric Environment 43, 697-705.

Woo, K.S., Chen, D.R., Pui, D.Y.H., McMurry, P.H., 2001. Measurement of Atlanta Aerosol Size Distributions: Observations of Ultrafine Particle Events. Aerosol Science and Technology 34, 75-87.

Wu, Z., Hu, M., Liu, S., Wehner, B., Bauer, S., Wiedensohler, A., Petäjä, T., Dal Maso, M., Kulmala, M., 2007. New particle formation in Beijing, China: Statistical analysis of a 1-year data set. Journal of Geophysical Research: Atmospheres 112, D09209, doi: 10.1029/2006JD007406.

Wu, Z., Hu, M., Lin, P., Liu, S., Wehner, B., Wiedensohler, A., 2008. Particle number size distribution in the urban atmosphere of Beijing, China. Atmospheric Environment 42, 7967-7980.

Yeung, L., To, W., 2008a. Size distributions of the aerosols emitted from commercial cooking processes. Indoor and Built Environment 17, 220-229.

Yeung, L.L., To, W.M., 2008b. Size distributions of the aerosols emitted from commercial cooking processes. Indoor Built Environment 17, 220-229.

Yue, D.L., Hu, M., Wang, Z.B., Wen, M.T., Guo, S., Zhong, L.J., Wiedensohler, A., Zhang, Y.H., 2013. Comparison of particle number size distributions and new particle formation between the urban and rural sites in the PRD region, China. Atmospheric Environment 76, 181-188.

Yue, W., Stölzel, M., Cyrys, J., Pitz, M., Heinrich, J., Kreyling, W.G., Wichmann, H.E., Peters, A., Wang, S., Hopke, P.K., 2008. Source apportionment of ambient fine particle size distribution using positive matrix factorization in Erfurt, Germany. Science of the Total Environment 398, 133-144.

Zhang, J.J., McCreanor, J.E., Cullinan, P., Chung, K.F., Ohman-Strickland, P., Han, I.-K., Jarup, L., Nieuwenhuijsen, M.J., 2009. Health effects of real-world exposure to diesel exhaust in persons with asthma. Research Report, Health Effects Institute, 5-109; Discussion 111-123.

Zhang, K.M., Wexler, A.S., 2004. Evolution of particle number distribution near roadways—Part I: analysis of aerosol dynamics and its implications for engine emission measurement. Atmospheric Environment 38, 6643-6653.

Zhang, K.M., Wexler, A.S., Zhu, Y.F., Hinds, W.C., Sioutas, C., 2004. Evolution of particle number distribution near roadways. Part II: the 'Road-to-Ambient'process. Atmospheric Environment 38, 6655-6665.

Zhang, R., Khalizov, A., Wang, L., Hu, M., Xu, W., 2011. Nucleation and growth of nanoparticles in the atmosphere. Chemical Reviews 112, 1957-2011.

Zhou, L., Hopke, P.K., Stanier, C.O., Pandis, S.N., Ondov, J.M., Pancras, J.P., 2005a. Investigation of the relationship between chemical composition and size distribution of airborne particles by

1566 partial least squares and positive matrix factorization. Journal of Geophysical Research:
1567 Atmospheres 110, D07S18, doi:10.1029/2004JD005050.

1568 Zhou, L., Kim, E., Hopke, P.K., Stanier, C., Pandis, S.N., 2005b. Mining airborne particulate size
1569 distribution data by positive matrix factorization. Journal of Geophysical Research: Atmospheres
1570 110, D07S19, doi:10.1029/2004JD004707.

1571 Zhou, L., Kim, E., Hopke, P.K., Stanier, C.O., Pandis, S., 2004. Advanced Factor Analysis on
1572 Pittsburgh Particle Size-Distribution Data Special Issue of Aerosol Science and Technology on
1573 Findings from the Fine Particulate Matter Supersites Program. Aerosol Science & Technology 38,
1574 118-132.

1575 Zhu, Y., Fanning, E., Yu, R.C., Zhang, Q., Froines, J.R., 2011. Aircraft emissions and local air
1576 quality impacts from takeoff activities at a large International Airport. Atmospheric Environment
1577 45, 6526-6533.

1578 Zhu, Y., Hinds, W.C., Kim, S., Shen, S., Sioutas, C., 2002a. Study of ultrafine particles near a
1579 major highway with heavy-duty diesel traffic. Atmospheric Environment 36, 4323-4335.

1580 Zhu, Y., Hinds, W.C., Kim, S., Sioutas, C., 2002b. Concentration and size distribution of ultrafine
1581 particles near a major highway. Journal of the Air & Waste Management Association 52, 1032-
1582 1042.

1583 Zhuang, Y., Biswas, P., 2001. Submicrometer particle formation and control in a bench-scale
1584 pulverized coal combustor. Energy & Fuels 15, 510-516.

1585

TABLE LEGENDS

Table 1: Overview of particle number size distributions generated from traffic emissions.

Table 2: Total number concentration at traffic sampling sites.

Table 3: Overview of particle number size distribution of brake wear particles.

Table 4: Particle size from industrial emissions.

Table 5: Particle sizes from cooking emissions.

Table 6: PMF studies in different cities.

Table 7: Uncertainty estimation.

Table 8: PNSD source profiles of particles reported in PMF analysis.

Table 9: Source apportionment of particle number in different cities.

FIGURE LEGENDS

Figure 1: A) Number, B) Surface, and C) Volume distribution for a typical urban background aerosol in North Kensington, London during 24^{th}-29^{th} July 2012.The APS/SMPS dataset was collected during the ClearfLo Project and merged by the authors.

Figure 2: Distribution of particles in the nucleation (Nu), Aitken (Aik) and accumulation (Acc) modes in different European sampling sites: COP: Copenhagen (Denmark); LEI: Leipzig (Germany); HEL: Helsinki (Finland); LON: London (UK), MAD: Madrid (Spain). BA denotes Urban background and RO denotes Urban roadside. Data is extracted from Von Bismarck-Osten et al. (2013) and Gómez-Moreno et al. (2011).

1620 Table 1: Overview of particle number size distributions generated from traffic emissions.

Vehicle type	Fuel type	Test method	Instruments	Size range	EF (particle /km)	NC (particle /cm^3)	Number Mode- (GSD)	References
Multipoint port injection- GS engine	GS	CDT	EEPS	5.5-560 nm	-	0.9-1.2E07	< 20 nm	Gupta et al. (2010)
	MD					2.9-8.8E07	> 40 nm	
LDV	GS	CDT	EEPS	5.5-560 nm	-	1.10E07	10.8 nm	Li et al. (2013)
		ORM				3.70E06	10.8/39.8 nm	
HDV EURO II bus	D	ORM	EEPS	5.5-560 nm	-	~ 6.5E07	~ 10 nm/140-160 nm	Armas et al. (2012)
	ED	ORM				~ 7.5E07	~ 10 nm/ 100-160 nm	
	EBD	ORM				~ 3.5E07	~ 10 nm/ 40-60 nm	
HDV	D	CDT	SMPS/ELPI	9.6 nm-10 um	-	1.00E08	< 25 nm at 1600 rev./min	Shi and Harrison (1999)
						6.00E07	40-60 nm at 2500 rev./min	
HDV EURO III	D	ORM	SMPS	7 -316 nm	-	-	10-20 nm/ 50 nm	Vogt et al. (2003)
	DLS	ORM			1.10E14		50 nm (1.8)	
	DLS	CDT			9.30E13		50 nm (1.7)	
HDV EUIII	D	ORM	SMPS	7-400 nm	~1.5E14	~8.5E06	70-100 nm	Wehner et al. (2009)
LDV EUIV	GS				~1.7E12	~1.6E05	15-20 nm/ 70-100 nm	
HDV	D	CDT	DMS/EEPS	4.5-1000 nm	-	-	60-100 nm	Biswas et al. (2008)
Vauxhall Astra Van	D	ORM	DMS	5-560 nm	-	~1.19E07	11-21 nm/ 63-112 nm	Carpentieri and Kumar (2011)
DV EUIII	D	CDT/ORM	SMPS	2.5-316 nm	-	-	10-20 nm/ 50-70 nm	Casati et al. (2007)
	DLS	CDT/ORM					50-70 nm	
DPC EUIII	D	CDT	SMPS	7.6- 300 nm	-	-	~10 nm/ 55-62 nm	Giechaskiel et al. (2005)
		ORM					~20 nm/ 60- 63 nm	
HDV EUIII	D	CDT	SMPS/FMPS	5.6- 560 nm	-	1E07-1E08	< 23 nm/ 50 nm	Giechaskiel et al. (2010)
HDV- bus	D	ORM	EEPS	5.6- 560 nm	7.06 E14		80 nm	Huang et al. (2013)
LDV-car	D	ORM			6.08 E14		60 nm	
LDV-car	GS	ORM			1.57 E14		20 nm	
Direct Injection	D	CDT	SMPS	12-604 nm	-	-	60-120 nm	Harris and Maricq (2001)

Port Injection	GS	CDT					40- 80 nm	
GDI	GS	CDT	ELPI	8 nm-10 um	1.84E12		23 nm	Liang et al. (2013)
GDI	MGS	CDT			8.46E11			
PFI	GS	CDT			5.39E11			
PFI	MGS	CDT			5.14E11			

Note: LDV: light duty vehicle; HDV: Heavy duty vehicle; DPS: Diesel passenger car; GDI: gasoline direct injected vehicle; PFI: Port fuel injected vehicle; GS: gasoline; D: diesel; MD: Mineral diesel; DLS: diesel low surful; ED: Ethanol/Diesel blends; EBD: Ethanol/Bio-diesel/Diesel blends; MGS: Methanol Gasoline; CDT: chassis dynamometer test; ORM: On-road measurements; EF: Emission factor; NC: number concentration (particle/cm3); GSD: Geometric Standard Deviation.

1637 Table 2: Total number concentration at traffic sampling sites.

Urban sites	City	Periods	Instruments	Size range (nm)	Peak number mode (nm)	Total counts (particle/cm^3)	References
RO	Raleigh, NC, US	Jul-Aug 2006	SMPS	20-1000	-	30000	Hagler et al. (2009)
RO	Beijing, China	Aug-07	SMPS	6-560	-	38400	Westerdahl et al. (2009)
RO	Kawasaki, Japan	Jan 2005	SMPS	10-470	20 nm	600000	Fushimi et al. (2008)
RO	New Delhi, India	Mar-Nov 2002	SMPS	3-800	-	50000	Mönkkönen et al. (2004)
RO	Santiago, Chile	Jul-Aug 2006	SMPS	10-700	20-30 nm	36300	Gramsch et al. (2009)
RO	El Paso, TX, US	Nov-Dec 1999	SMPS	20-100	-	14100	Noble et al. (2003)
TT	San Francisco, US	Jul-Aug 2006	SMPS	10-290	10-30 nm	200000	Ban-Weiss et al. (2010)
TT	California, US	Jul-Aug 1997	CNC	-	-	270000	Kirchstetter et al. (1999)
TT	Sydney. Australia	May-July 2006	CPC	10-1000	-	100000	Knibbs et al. (2009)
TT	Rouen, France	May 2002	ELPI	30-10000	< 60 nm	95000	Gouriou et al. (2004)
SC	Copenhagen, Denmark	May-Nov 2001	DMPS	10-700	20-25 nm	21400	Ketzel et al. (2003)
SC	Leipzig, Germany	Oct-Dec 1997	TDMPS	3-800	15 nm	110000	Wehner et al. (2002)
SC	Shanghai, China	May, Nov 2005	SMPS	10-487	10-30 nm	120000	Li et al. (2007)
SC	Manchester, UK	Oct 2001	SMPS	4-160	25-30 nm	27000	Longley et al. (2003)
Near HW	Los Angeles, CA, US	Aug-Oct 2001	SMPS	6-220	10-20 nm	180000	Zhu et al. (2002a)
Near HW	Toronto, Canada	Aug-04	CPC-GRIMM	-	-	33867	Beckerman et al. (2008)
HW (100 m)	Brisbane, Australia	1995-1999	SMPS	16-700	40-60 nm	7400	Morawska et al. (2002)
Near HW	Cassino, Italy	Apr-May 2004	SMPS, APS	6-20000	7-30 nm	190000	Buonanno et al. (2009b)
On HW	Minnesota, US	Nov-2000	SMPS	8-300	14-30 nm	403000	Kittelson et al. (2004)
SW station	Helsinki, Finland	Mar 2004	DMPS	10-500	-	31000	Aarnio et al. (2005)

1638 *Notes:* RO: Roadside; TT: Traffic Tunnels; SC: Street Canyon; HW: Highway; SW: Subway
1639
1640

1641 Table 3: Overview of particle number size distribution of brake wear particles.

1642

Brake testing	Vehicle type	Brake Type	Pad/shoes	Instruments	Size range	Diameter	Number mode (μm)		References
							Major	Minor	
Field	Gasoline car	Disc (grey cast iron)	LM	GRIMM	0.25-32	Optical	0.35-0.40	-	Wahlström and Olofsson (2015)
Field	Train	Disc	-	GRIMM	0.25-32	Optical	0.28; 0.35	0.6; 3-6	Abbasi et al. (2012b)
Field	Diesel car	Disc	-	EEPS	0.06-0.56	Mobility	0.01	-	Mathissen et al. (2011)
Field/Road simulation	Gasoline car	Disc	NAO	FMPS	0.05-0.52	Mobility	0.01	-	Kwak et al. (2014)
Dynamometer	-	Disc/drum	SM	MOUDI/ELPI	0.1-18	Aerodynamic	< 30 nm	-	Garg et al. (2000)
Dynamometer	Light duty	Disc	LM/SM/NAO	MOUDI/ELPI	0.1-18	Aerodynamic	1-2	-	Sanders et al. (2003)
Dynamometer	Passenger cars	Disc (grey cast iron)	LM	SMPS	0.01-0.45	Mobility	0.1	0.3	Kukutschová et al. (2011)
				APS	0.5-20	Aerodynamic	1.5-2	-	
Pin-on-dics	Truck	Disc (grey cast iron)	SM	LA700	0.04-262	Optical	0.35	2-7-15	Mosleh et al. (2004)
Pin-on-dics	Passenger cars	Grey cast iron	LM/NAO	GRIMM	0.25-32	Optical	0.35	0.28; 0.55	Wahlström et al. (2010a)
				SMPS	0.01-0.52	Mobility	0.1	-	
Pin-on-dics	Train	railway wheel	cast iron/ composition brake block	GRIMM	0.25-32	Optical	~ 0.3	0.28; 0.6	Olofsson (2011)
				SMPS	0.01-0.52	Mobility	0.07	-	
Pin-on-dics	Train	railway wheel	Organic/Sintered /Cast iron/Steel	GRIMM	0.25-32	Optical	0.3-0.4	0.5-0.6; 3-6	Abbasi et al. (2012a)
				SMPS	0.01-0.52	Mobility	0.07-0.12	-	
Test rig	-	Disc	LM / NAO	GRIMM	0.25-32	Optical	0.35	0.6; 3	Wahlström et al. (2009)
Test rig	-	Disc	LM / NAO	APS	0.5-20	Aerodynamic	1-2	-	Iijima et al. (2007)
Test rig	-	Disc	NM/ NAO	APS	0.5-20	Aerodynamic	0.8	-	Iijima et al. (2008)

1643 Note: LM: Low metallic; NAO: Semi-metallic; NAO: Non-asbestos organic;

1644

1645

1646

1647 Table 4: Particle size from industrial emissions.

Methods	Combustion system	Fuels	Method	Size range	NM-1 (nm)	NM-2 (nm)	References
Flue gas	Power plant	pulverized coal	DMA	0.01-1	0.04	0.3	Joutsensaari et al. (1992)
Flue gas	Combustor -laboratory scale	pulverized coal	ELPI/SMPS	0.01-10	0.07	-	Li et al. (2009)
Flue gas	Combustor -laboratory scale	pulverized bituminous coal	SMPS	-	0.06-0.09	-	Zhuang and Biswas (2001)
Flue gas	Combustor -laboratory scale	Pulverized sub-bituminous coal	SMPS	0.01-0.5	0.03-0.05	~0.3	Suriyawong et al. (2006)
Stack plume	Pilot-Scale Combustor	Low sulphur bituminous coal	SMPS/APS	0.003-20	0.01	0.05	Lipsky et al. (2002)
Flue gas	Coal-Fired Power Plant	pulverized coal	ELPI	0.03-10	-	0.08	Ohlström et al. (2000)
Flue gas	Coal-Fired Power Plant	pulverized coal	EEPS/APS	0.056-10	0.009	0.06; 0.835	Wang et al. (2008)
Flue gas	Pilot-scale test combustor	Coal	SMPS	0.01-0.4	0.04-0.06	-	Chang et al. (2004)
		Heavy Fuel Oil			0.07-0.10		
		Natural gas			0.015-0.025		
Stack plume	Package boiler	Oil shale	SMPS	0.013-0.083	0.020-0.028	0.043-0.061	Morawska et al. (2006)
Field					0.027	0.05	
Flue gas	Municipal Waste Incineration Plant	-	SMPS/APS	0.017-30	0.04	0.090-0.140	Maguhn et al. (2003)
Stack plume					ULD	0.04-0.07	
Stack plume	Municipal waste-to-energy (WTE) plants	-	ELPI	0.007-10	0.017-0.035	0.08	Cernuschi et al. (2012)
Stack plume	Municipal waste incinerator	-	ELPI	0.03-10	-	0.08	Buonanno et al. (2009a)

1648 NM: number mode (nm).

Table 5: Particle sizes from cooking emissions.

Activities			NPV (part/cm3)	NMD (nm) (GSD)	Sampling equipment	References
Grilling	gas stove at maximum power	Cheese	1.10E+05	41	APS, SMPS (6nm-20 um)	Buonanno et al. (2009c)
		Wurstel	1.30E+05	43		
		Eggplants	1.20E+05	29		
		Bacon	1.00E+05	49		
	gas stove at minimum	Bacon	-	22		
Frying	gas stove at maximum power	chips with Olive oil	1.20E+05	61.5 (1.91)		
		chips with Peanut oil	1.20E+05	49.6 (1.82)		
		chips with Sunflower oil	1.10E+05	49.6 (1.80)		
Rings	Gas	No Food	2.60E+04	16	SMPS (10-500 nm)	Dennekamp et al. (2001)
	Electric	No Food	9.40E+04	32		
	Gas	Boil water	1.33E+05	17		
	Gas	Stir fry	1.37E+05	41		
	Electric		1.10E+04	22		
	Gas	Fry bacon	5.90E+05	69		
	Electric		1.59E+05	72		
Oven	Gas	Bake cake	9.80E+04	34		
	Electric		3.00E+04	38		
	Gas	bake potatoes	1.25E+05	39		
	Electric		1.60E+04	46		
Grill	Gas	No Food	1.03E+05	24		
	Electric		7.70E+04	20		
	Gas	Toast	1.38E+05	25		
	Electric		1.34E+05	27		
	Gas	Bacon	4.13E+05	39		
	Electric		5.30E+05	53		
Cooking			1.26E+05	22-63	APS, SMPS (15nm-20 um)	He et al. (2004)
Cooling pizza			1.37E+05			
Frying			1.54E+05			
Grilling			1.61E+05			
Kettle			1.56E+04			
Microwave			1.63E+04			
Oven			6.15E+04			
Stove			1.79E+05			
Toasting			1.14E+05			

Cooking		-	20-70	SMPS	Abt et al. (2000)
Electric oven		1.80E+06	20-100	SMPS (14-552 nm)	Hussein et al. (2006a)
Gas stove	scrambling eggs	1.80E+05	40 (2.1)	SMPS (17-886 nm)	Li et al., 1993
	frying chicken	2.60E+05	50 (1.86)		
	cooking soup	1.00E+05	30 (1.8)		
Gas stove	Steaming	5.40E+04	<10; 70-80	SMPS (10-500 nm)	See and Balasubramanian (2006)
	Boling	6.90E+04	<10; 70-80		
	Stir-frying	9.30E+04	10-25		
	Pan-frying	1.10E+05	10-25		
	Deep-frying	5.95E+05	10-25		
Chinese style using gas stove		8.98E+06	140 (1.63)	SMPS (16-674 nm)	Yeung and To (2008a)
Western style using electric griddle		8.83E+05	100-160 (2.6)		
Hot oil test		6.47E+05	107 (3.0)		
Frying tortillas-gas stove			<10; 60	SMPS (10-1000); APS	Wallace (2006)

NPV: number peak value; NMD: number mode diameter; GSD: geometric standard deviation

Table 6: PMF studies in different cities.

Sampling Sites	Size Range	Methods	No. of factors	References
Brisbane, Australia	14 nm-0.7 µm	SMPS	6	Friend et al. (2012)
Reston, VA, USA	10 nm-20 µm	APS/SPMS	9	Ogulei et al. (2006a)
Baltimore, USA	10 nm-2.5 µm	APS/SPMS	12	Ogulei et al. (2006b)
Rochester, NY, USA	12 nm-0.5 µm	SMPS	10	Ogulei et al. (2007)
Prague, Czech	15 nm-0.7 µm	SMPS	4	Thimmaiah et al. (2009)
Seattle, WA, USA	20 nm-0.6 µm	DMPS	4	Kim et al. (2003)
Augsburg, Germany	3.8 nm-8.8 µm	DMA, APS	6	Gu et al. (2011)
Rochester, NY, USA	11nm-0.5 µm	SMPS	7-9	Kasumba et al. (2009)
Pittsburgh, USA	3 nm-2.5 µm	SMPS/APS	5	Zhou et al. (2004)
Erfurt, Germany	10 nm-3 µm	DMPS/LAS-X	5	Yue et al. (2013)
Beijing, China	3 nm-0.9 µm	TDMPS	4	Wang et al. (2013)
London, UK	15 nm-18 µm	APS/SPMS	10	Harrison et al. (2011)

Table 7: Uncertainty estimation.

PMF uncertainties for particles	References
$\sigma_{i,j} + C_3(N_{i,j})$	Ogulei et al. (2006a)
$\sigma_{i,j} + C_3 \max(\lvert N_{i,j}\rvert, \lvert Y_{i,j}\rvert)$	Zhou et al. (2005a)
$1 + \sqrt{N_{i,j}} + 0.1 \times (N_{i,j})$	Thimmaiah et al. (2009)
$\frac{5}{6}$ x MDL if $N_{i,j} \leq$ MDL $\sqrt{(Error\ Fraction\ x\ N_{i,j})^2 + MDL^2}$ if $N_{i,j} >$ MDL	Wang et al. (2013)

Notes: $\sigma_{i,j}$ is the calculated measurement error for size bin j and sample i. $N_{i,j}$ is the measured number concentration for size bin j and sample i. C_3 is a dimensionless constant value and should be chosen in which the scaled residuals are approximately randomly distributed between -2 to +2. Ogulei et al. (2006a) reported that the value of C3 ranges from 0.01 to 0.5, with a value of 0.4 providing the best results with the PMF model. $Y_{i,j}$ is the calculated value for $N_{i,j}$. Zhou et al (2005a) used a value of 0.08 for the C3 constant. MDL is method detection limit. Error fraction was estimated to be 15 for small particles (Dp< 25nm) and 10 for larger particles (Thimmaiah et al, 2009).

Table 8: PNSD source profiles of particles reported in PMF analysis.

Sources	**Mode (nm)**	**Correlation with air pollutants**	**Diurnal Profiles**	**References**
Petrol vehicles	30-40	NO, PM_{10}, CO	05-08. AM & 05-06. PM	Friend et al. (2013)
Diesel vehicles	50-80	NO. CO	05-08. AM & 06-12. PM	
Aircraft	15-20	NO, NO_2 PM_{10}, CO	05-08. AM	
Biomass burning	100-200	NO, PM_{10}	Morning, Evening	
Nucleation 1	5-10	-	Morning, afternoon	Ogulei et al. (2007)
Nucleation 2	Multips	SO_2	Mid afternoon	
Local traffic	20-30	-	Pronounced morning	
Distant traffic	50-80	CO, $PM_{2.5}$	Evening	
Industrial Emissions	40-50	-	-	
Residential/ Commercial Heating	100-200	$PM_{2.5}$, CO	Evening	
Secondary Nitrate	200-300	$PM_{2.5}$	Evening	
O3-rich secondary aerosol	Mutips	O_3	Daytime, Summer	
Secondary Sulphate	100-200	$PM_{2.5}$	-	
Regional Transport	200-300	$PM_{2.5}$	-	
Re-suspended dust	-	Ca, Mg, Fe,Ni,Mn,Cr,Ti, Co	Daytime	Gu et al. (2011)
Fresh traffic	9-10		Morning rush hours	
Aged traffic	20-100	OC, EC, NO_2,NO,Cu,Sb,Ce	Morning rush hours/evening	
Stationary combustion	70-80	OC, EC, NO, NO_2	Morning/nigh time	
Long-range transported dust	0.7-3um	NH_4, NO_3		
Nucleation	5.5		rush hours	
Secondary aerosol	320	NH_4,SO_4, EC, OC	Night time	
Regional secondary	300	$PM_{2.5}$, SO_4		Zhou et al. (2004)
Diesel emission	40	NOx, CO, EC		
Local traffic	15	-	rush hours	
Combustion	100	NO, NOx, CO, EC		
New particles	3	-	mid and late afternoon	
Airborne soil	1-2.84um	No correlation	Moderate	Yue et al. (2008)
Local traffic	10-100	NO, NO_2, CO, OC, EC	Strong	

Secondary aerosols from local fuel traffic	0.25-1.8 um	NO_2, CO, OC, EC	Weak	
Remote traffic	10-500	CO,SO_2, OC, EC	Strong	
Secondary aerosols from multiple sources	0.2-1.0 um	SO_4, OC, EC	Weak	
Local traffic	16	NOx	morning/evening	Wang et al. (2013)
Remote traffic	50		after rush hours	
Combustion	100	BC		
Secondary transformation	30	SO_4, NO_3,NH_4, Oxygenated organic aerosol		

Table 9: Source apportionment of particle number in different cities (%).

	Pittsburgh, NY,US	Rochester, NY,US	Barcelona, Spain	Augsburg, Germany	Beijing, China
Nucleation	-	24.5	3.3	3.7	-
Local traffic	21.7	21.9	64.2	24.9	25
Distant traffic	20	16		40.3	29
Industry	-	20.3	1.8	-	-
Secondary nitrate	28.2	1	-	1.2	33
Secondary sulphate		6.2	-		
Regional transport	9	1.5	24.2	-	-
Combustion	21.1	-	0.3	26.1	13
Re-suspension	-	-	1.4	2.6	-
Residential heating	-	6.6	-	-	-
Others	-	1.7	1.8	-	-
	Zhou et al. (2004)	Ogulei et al. (2007)	Pey et al. (2009)	Gu et al. (2011)	Wang et al. (2013)

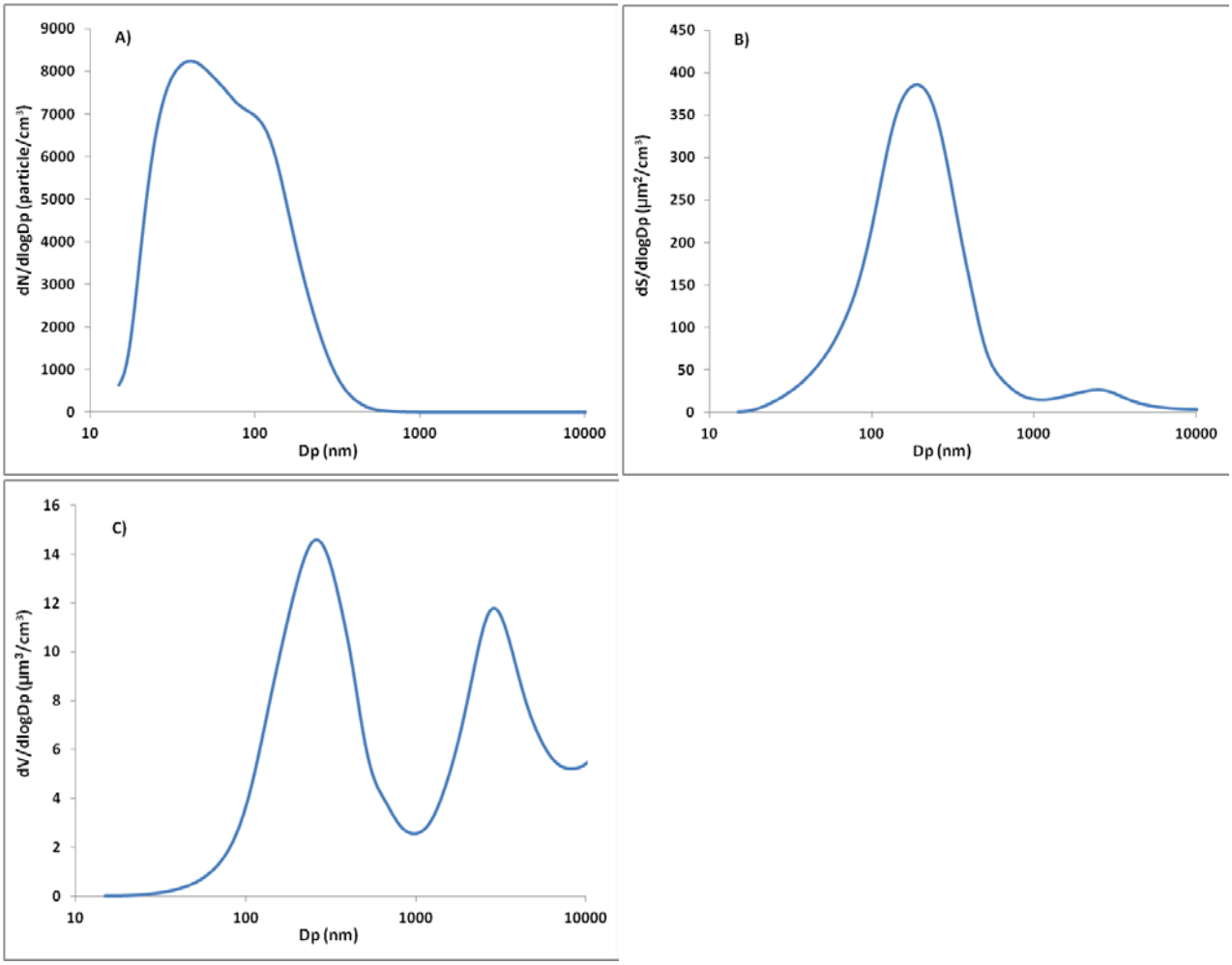

Figure 1: A) Number, B) Surface, and C) Volume distribution for a typical urban background aerosol in North Kensington, London during 24th-29th July 2012.The APS/SMPS dataset was collected during the ClearfLo Project and merged by the authors.

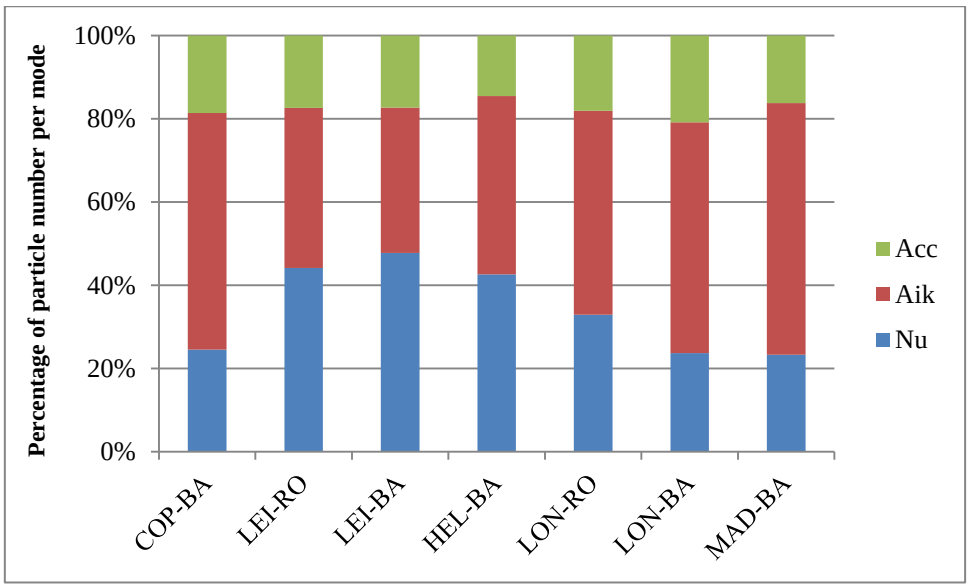

Figure 2: Distribution of particles in the nucleation (Nu), Aitken (Aik) and accumulation (Acc) modes in different European sampling sites: COP: Copenhagen (Denmark); LEI: Leipzig (Germany); HEL: Helsinki (Finland); LON: London (UK), MAD: Madrid (Spain). BA denotes Urban background and RO denotes Urban roadside. Data is extracted from Von Bismarck-Osten et al. (2013) and Gómez-Moreno et al. (2011).